AD_____

Award Number: W81XWH-12-2-0091

TITLE: Maintenance of Paraoxonase 2 Activity as a Strategy to Attenuate P. Aeruginosa Virulence

PRINCIPAL INVESTIGATOR: John Teiber

CONTRACTING ORGANIZATION: The University of Texas Southwestern Medical Center
Dallas, TX 75390

REPORT DATE: October 2014

TYPE OF REPORT: Annual Report

PREPARED FOR: U.S. Army Medical Research and Materiel Command
Fort Detrick, Maryland 21702-5012

DISTRIBUTION STATEMENT: Approved for Public Release;
Distribution Unlimited

The views, opinions and/or findings contained in this report are those of the author(s) and should not be construed as an official Department of the Army position, policy or decision unless so designated by other documentation.

REPORT DOCUMENTATION PAGE

Form Approved
OMB No. 0704-0188

1. REPORT DATE	2. REPORT TYPE	3. DATES COVERED
October 2014	Annual Report	30 Sep 2013 - 29 Sep 2014

4. TITLE AND SUBTITLE
Maintenance of Paraoxonase 2 Activity as a Strategy to Attenuate P. Aeruginosa Virulence.

5a. CONTRACT NUMBER

6. AUTHOR(S)
Teiber, John, F.
E-Mail: john.teiber@utsouthwestern.edu

5d. PROJECT NUMBER
W81XWH-12-2-0091

5f. WORK UNIT NUMBER

7. PERFORMING ORGANIZATION NAME(S) AND ADDRESS(ES)
University of Texas Southwestern Medical Center
5323 Harry Hines Blvd.
Dallas, Texas, 75390

UNIVERSITY MEDICAL CENTER MAINZ
Institute of Pharmacology
Obere Zahlbacher Str. 67, 55131 Mainz, Germany

8. PERFORMING ORGANIZATION REPORT NUMBER

9. SPONSORING / MONITORING AGENCY NAME(S) AND ADDRESS(ES)
U.S. Army Medical Research and Materiel Command
Fort Detrick, Maryland 21702-5012

10. SPONSOR/MONITOR'S ACRONYM(S)

11. SPONSOR/MONITOR'S REPORT NUMBER(S)

12. DISTRIBUTION / AVAILABILITY STATEMENT
Approved for Public Release; Distribution Unlimited

13. SUPPLEMENTARY NOTES

14. ABSTRACT
The *P. aeruginosa* signaling and virulence molecule 3OC12 mediates inactivation of the lactonase paraoxonase 2 (PON2) and induces many immunomodulatory effects in host cells. Because PON2 rapidly inactivates 3OC12, we hypothesized that preventing PON2 inactivation by 3OC12 could be a therapeutic strategy to limit *P. aeruginosa* quorum signaling and thereby attenuate virulence. In human and mouse primary cell types we found PON2 to be sensitive to 3OC12-mediated inactivation at concentrations of 3OC12 expected to be present near *P. aeruginosa* colonies during infection. We also discovered that 3OC12 is rapidly hydrolyzed intracellularly by PON2 to 3OC12-acid, which becomes trapped and accumulates within the cells, specifically within the endoplasmic reticulum and mitochondria. 3OC12 caused a rapid PON2-dependent cytosolic and mitochondrial pH decrease, calcium release and phosphorylation of stress signaling kinases. The findings suggest that intracellular acidification is the proximal event that mediates many immunomodulatory effects of 3OC12 and PON2 inactivation. PON2 appears to be inactivated by 3OC12 via an endoplasmic reticulum stress like response triggered by acidification. Two compounds were identified that inhibit both intracellular acidification and PON2 inactivation, suggesting that they could be developed as potential drugs to prevent 3OC12-mediated biological effects. Protecting cells from 3OC12-mediated acidification could be an important therapeutic strategy to attenuate *P. aeruginosa* quorum signaling and virulence as well as host cell immunomodulation.

15. SUBJECT TERMS
Acyl-homoserine Lactone, Bacterial Pathogenesis, Host Defense, Host-Pathogen Interactions, Innate Immunity, Paraoxonase, *Pseudomonas aeruginosa*, Quorum Sensing

16. SECURITY CLASSIFICATION OF:			17. LIMITATION OF ABSTRACT	18. NUMBER OF PAGES	19a. NAME OF RESPONSIBLE PERSON
a. REPORT	b. ABSTRACT	c. THIS PAGE			USAMRMC
U	U	U	UU	35	19b. TELEPHONE NUMBER *(include area code)*

I. Table of Contents

II. Introduction

3OC12 is an important autocrine signaling molecule produced by *P. aeruginosa* that has been shown to be required for full *P. aeruginosa* virulence in animal models of infection. Cellular PON2 hydrolyzes, and thereby inactivates 3OC12, and is considered a potential important host defense that limits *P. aeruginosa* pathogenicity. We previously demonstrated that 3OC12 can rapidly inactivate cellular PON2. Thus, we proposed in our grant proposal that preventing PON2 from becoming inactivated by 3OC12 could be a viable therapeutic strategy to attenuate *P. aeruginosa* pathogenicity without causing drug resistance. A primary goal of the project, as described in Aim 1 of the proposal, was to identify the mechanisms by which PON2 was inactivated by 3OC12 and identify potential compounds that could block this inactivation. An additional goal, as described in Aim 2 of the proposal, was to demonstrate that PON2 was susceptible to 3OC12-mediated inactivation in primary cell types relevant to infection and in vivo in mice. During the course of our investigations we discovered a novel PON2-dependent mechanism by which 3OC12-mediates host cell biological effects. Given that many of the effects of 3OC12 on host cells are believed to undermine the host's immune response, we also further characterized this new mechanism as an additional goal to better understand *P. aeruginosa*-host interactions.

Key Words: Acyl-homoserine Lactone, Bacterial Pathogenesis, Host Defense, Host-Pathogen Interactions, Innate Immunity, Paraoxonase, *Pseudomonas aeruginosa,* Quorum Sensing

III. Results

Aim 1

Discovery of a novel PON2-dependent mechanism that mediates 3OC12 biological effects in host cells.

In year 1 we discovered a novel mechanism by which PON2 hydrolyzes 3OC12 to 3OC12-acid, which becomes trapped and accumulates intracellularly. This results in a rapid intracellular acidification which initiates immediate cell biological responses. This initial discovery was detailed in a short manuscript that was submitted to The Journal of Biological Chemistry last year (see Year 1 Annual Report). The manuscript was not accepted and the editor suggested resubmitting after additional experiments were performed. Per the editor's suggestion, additional experiments were performed and a greatly expanded and revised version of the manuscript was submitted to The Journal of Biological Chemistry and is currently under review. The complete manuscript including that data, figures and a detailed discussion of the mechanism and significance of the findings can be viewed in appendix I of this report.

Progress towards identification of the mechanism by which 3OC12 mediates PON2 inactivation in year 2.

Calcium signaling does not cause 3OC12-mediated PON2 inactivation – Our original hypothesis was that 3OC12 induced a calcium-dependent activation of calmodulin/calcineurin (CN) which dephosphorylated PON2, resulting in inactivation. We subsequently demonstrated (see Year 1 Annual Report) that PON2 is phosphorylated on serine 36, but dephosphorylation at this site is not causing 3OC12-mediated inactivation. Using inhibitory RNA techniques, we demonstrated that calmodulin was not involved in PON2 inactivation. This year we completed the inhibitory RNA studies (Aim 1, subtask 4c) demonstrating that knockdown of CN also does not affect 3OC12-mediated PON2 inactivation (Fig 1). Together these findings indicate PON2 is not inactivated via the calcium/calmodulin/CN dephosphorylation pathway.

Because 3OC12 induces a rapid calcium cytosolic increase we further explored a potential role for calcium signaling in PON2 inactivation. Cells were treated with the calcium mobilizers ATP and the phospholipase C activator m3MFBS. ATP can induce cytosolic calcium increase via gated ion channels or metabotropic G-protein coupled receptors. m3MFBS generates inositol phosphate and subsequent release of intracellular calcium from the endoplasmic reticulum (ER). Treatment of human bronchial epithelial cells (HBEC) with ATP resulted in a very rapid and large increase in calcium that recovered to initial levels within 15 minutes (Fig. 2A). However, ATP was unable to mediate the inactivation of PON2 (Fig. 2B). m3M3FBS induced an almost identical calcium response as 3OC12 (Fig 2A), yet resulted in little to no PON2 inactivation

(Fig. 2B). When A549 cells were treated with 200 μM ATP, kinetics of cytosolic calcium increase were almost identical to the HBECs, yet it didn't inactivate PON2 (data not shown). Treatment of A549 cells with 25 μM m3M3FBS was also unable to inactivate PON2 (data not shown). These findings suggest that signaling due to cytosolic calcium increase does not mediate PON2 inactivation.

Acidification is the proximal event that triggers PON2 inactivation – Our discovery of a rapid PON2-dependent accumulation of 3OC12-acid and acidification within the ER and mitochondrial (see appendix I), suggested that acidification within these organelles is the proximal event that triggers PON2 inactivation by 3OC12. We also previously demonstrated that W7 a calmodulin inhibitor, could protect PON2 from 3OC12-mediated inactivation. Because we ruled out calmodulin mediating PON2 inactivation, and W7 is a weak base, we hypothesized that it protects PON2 from inactivation by preventing intracellular acidification by 3OC12. Indeed, W7 very efficiently prevented 3OC12-mediated intracellular acidification (Fig 3A). Like W7, sphingosine is also a weak base that can inhibit calmodulin. Sphingosine also prevented 3OC12-mediated intracellular acidification and PON2 inactivation (Fig 3B and C). The findings corroborate acidification as the initiating event that causes PON2 inactivation and provides potential model therapeutic compounds to prevent PON2 inactivation.

Maintenance of appropriate pH within the cell is critical to cell functions. Therefore, cells stringently regulate intracellular pH by employing diverse families of proton extruders and pumps and a balance of intracellular weak acids and bases to increase buffering capacity(1). To provide corroborating evidence for an acidification-dependent mechanism mediating PON2 inactivation we employed an approach of disrupting the ability of the cells to regulate pH recovery before 3OC12 treatment. We tested cariporide, a Na^+/H^+ exchange inhibitor, to see if it would potentiate PON2 inactivation by 3OC12. Cariporide appeared to have no effect on 3OC12-mediated PON2 inactivation (Fig 4). Cariporide also had little effect on cytosolic pH, either when cells were treated with or without 3OC12 (data not shown). While the findings are not consistent with our hypothesis they don't contradict it either. Cells employ a broad range of pH regulating mechanisms and it is likely that cariporide alone does not prevent pH drop, or effect pH, to an extent necessary to affect PON2 inactivation. We are currently employing more extreme techniques to prevent pH recovery, or potentiate pH drop, such as co-treatment with cariporide and inhibitors of other pH regulating mechanisms to determine if they will potentiate 3OC12-mediated PON2 inactivation.

PON2 is not directly inactivated by low pH and low calcium – Our demonstration that acidification is the proximal event that causes PON2 inactivation, and our findings that calcium signaling does not cause PON2 inactivation, led us to hypothesize that pH drop, and/or calcium depletion in the ER, is causing a "direct" denaturation of PON2, resulting in irreversible inactivation. PON proteins require calcium both for hydrolytic activity and for stability(2). To test PON2 stability, we treated A549 cell lystates, which express high levels of PON2, with decreasing concentrations of calcium under acidic conditions for 10 minutes and then analyzed them for PON2 activity. As shown in Figure 5, PON2 still maintained 40% of its activity after treatment at pH 4.5 and 1 μM calcium. PON2 is inactivated by over 90% after treatment of cells with 3OC12. Thus, the data suggest that if PON2 is becoming inactivated via pH dependent denaturation, the combined pH and calcium concentrations must be below 4.5 and 1 μM within the ER and the mitochondria, where PON2 resides, after 3OC12 treatment of cells. While it is possible such extreme conditions are reached in these compartments after 3OC12 treatment of cells with 3OC12, the ability of cells to maintain pH makes it seem unlikely that such a denaturation mechanism is responsible for PON2 inactivation.

PON2 inactivation appears to be induced by an ER stress pathway – Thapsigargin inhibits the sarco/endoplasmic reticulum calcium-ATPase pumps in the ER, resulting in a rapid depletion in luminal ER calcium, and corresponding cytosolic calcium rise. Surprisingly, treatment of A549 cells with thapsigargin for 15 minutes resulted in > 90% inactivation of PON2 (Fig. 6). The same thapsigargin treatment of HEK PON2 GFP cells also resulted in > 90% inactivation of PON2 (data not shown). Because thapsigargin is very unlikely to cause dramatic intracellular acidification (i.e. < pH 4.5), it suggests that PON2 is not inactivated by an acidification/calcium-dependent denaturation. This suggests that both thapsigargin and 3OC12 (via PON2-dependent acidification) may rapidly induce an ER stress like response that mediates PON2 inactivation.

Using protein crosslinking agents followed by separation of crosslinked bands by PAGE we identified a PON2 protein crosslinked complex of about 300 kD that forms after treatment of cells with 3OC12 (see Year 1 Annual Report). This year we were able to immunoprecipitate the crosslinked protein, separate it by PAGE, cut

out the appropriate size band (Fig 7) and have it analyzed by mass spectrometry at the UTSW proteomics core facility. The highest scoring protein was human GRP78 (see appendix II). This protein has a molecular mass of 78 kD. GRP78 (also known as BiP) is a molecular chaperone of the heat shock (HS) 70 protein family located in the lumen of the endoplasmic reticulum (ER). Together GRP78 and PON2-GFP would have a mass of ~ 150. Purified PON2 has been shown to exist in multimeric states and a crosslinked GRP78-PON2GFP dimer would be expected to be around 300 kD. Two additional HSP70 proteins were identified by mass spectrometry in the protein complex (see appendix II). To provide confirmatory evidence, HEK-PON2 overexpressing cells were treated with or without 3OC12, lysed, crosslinked and analyzed by Western analysis using a GRP78 specific antibody. GRP78 was identified in the ~300 kD crosslinked complex, confirming the presence of GRP78 in the complex (Fig. 8).

Epigallocatechin gallate (EG) is a reported inhibitor of GRP78. A549 cells were treated with 25 μM EG for 15 mins, or 250 μM EG overnight, followed by 100 μM 3OC12 for 10 minutes. EG had no effect on 3OC12-mediated PON2 inactivation (data not shown). This does not support a role for GRP78 in PON2 inactivation, however, we have no way of verifying that GRP78 was blocked by EG. Thus, weather GRP78 is inactivation PON2 or not requires more investigation. EG treatment alone also had no effect on PON2 activity. GRP78 expression is known to be induced by growing cells in glucose free media. To test the effect of increased GRP78 levels on PON2 inactivation, A549 cells were grown for 24 hours in either regular media or glucose free media to induce GRP78. As shown in Fig 9A, GRP78 was induced by growing in glucose free media. Densitometric analysis of the blot shown in Figure 9A showed that GRP78 expression was increased by 78 ± 26% in the cells grown in no glucose media. The increase in GRP78 had no effect on 3OC12-mediated PON2 inactivation (Fig. 9B).

The potential role of GRP78 in promoting PON2 activity recovery after 3OC12-mediated inactivation was also explored. We have shown that after 3OC12 treatment PON2 activity recovers before more PON2 protein is expressed, indicating inactivated PON2 can become reactivated(3). Cells were grown in standard media or glucose free media to induce GRP78. Cells were then treated with 3OC12 for 10 min and either collected immediately or allowed to recover for 3 hours in media free of 3OC12. Despite increased GRP78 levels in the cells grown in glucose free media (Fig. 10A), there was no significant increase in the rate of recovery of PON2 activity after 3OC12 treatment (Fig. 10B). The data suggests that if GRP78 is assisting in the refolding/recovery of activity PON2, the basal levels of GRP78 are sufficient to provide the maximum rate of refolding and additional GRP78 does not increase PON2 reactivation.

Aim 2 Task 1

3OC12 mediated down regulation of PON2 mRNA and protein – In addition to rapid inactivation of PON2, 3OC12 has also been shown to decrease PON2 mRNA and protein in cell lines(3). Under Aim 2, subtask 1, we demonstrated this year that PON2 mRNA and protein is also down regulated in primary HBEC, cells that come in direct contact with *P. aeruginosa* during pulmonary infection (Fig 11).

3OC12-mediated PON2 inactivation in mouse primary spleen cells – We previously demonstrated that PON2 was very sensitive to 3OC12-mediated inactivation in a range of primary cell types (see Year 1 Annual Report). We continued characterizing the sensitivity of different cell types to 3OC12-mediated PON2 inactivation. Freshly isolated mouse spleens contain predominantly lymphocytes, immune cells relevant to bacterial infection, that are easy to isolate. There was a non-significant trend in PON2 inactivation by 100 μM 3OC12 at 1 hour, although no inactivation was apparent at 2 hours treatment time (Fig. 12A). PON2 protein was expressed in the spleen cells (Fig. 12B) and the PON2 activity in the lysates was 6.4 ± 0.8 nmol/min/mg of lysate, validating that the cell express PON2. The findings suggest that PON2 is relatively refractive to 3OC12 mediated inactivation in the mouse spleen cells, possibly due to a stringent regulation of intracellular pH or lower levels of PON2 hydrolytic activity. Thus, this data, in combination with our previous data in other cell types, suggests significant variability in the sensitivity of PON2 to inactivation depending on cell type.

Aim 2 Task 2

Direct perfusion of mouse lung and liver with 3OC12 does not inactivate tissue associated PON2, but does result in accumulation of 3OC12-acid within the cells – Our previous approach of administering an aerosol of 3OC12 to the lungs of mice using the Microsprayer device did not result in any PON2 inactivation or

down regulation (see Year 1 Annual Report). This year we pursued a new approach to determine if 3OC12 had the capacity to inactivate PON2 in vivo. Anesthetized mice were perfused through the left ventricle with 8 ml of media containing 5% FBS with or without 200 µM 3OC12. The lungs were also filled, through the trachea, with 2 ml of the media with or without 200 µM 3OC12. One hour later the lungs were harvested, cut into sections and frozen. Frozen sections were then analyzed for PON2 activity. Although our sample number was low, this preliminary experiment indicated that no apparent inactivation of PON2 was observed using this ex vivo perfusion method (Fig 13A). To determine if 3OC12-acid was indeed being generated in the cells of the lung after perfusion, sections of the lung were homogenized in pH 5 MES buffer and extracted with acetonitrile/ethyacetate and extracts conjugated with the carboxylic acid conjugating agent PDAM according to the published protocol(5). PDAM conjugates were analyzed by HPLC. Although there was variability in the data, findings suggest that 3OC12-acid is accumulating in the lungs after 3OC12 perfusion (Fig 13B).

A similar preliminary experiment was performed in the liver, a highly perfused organ that is known to express relatively high levels of PON2. Anesthetized mice were perfused through the inferior vena cave with 20 ml of media containing 5% FBS with or without 200 µM 3OC12. One hour later the liver was harvested, cut into sections and frozen. Frozen sections were then analyzed for PON2 activity. Data show a trend of a decrease in PON2 activity in the 3OC12 treated livers (Fig 14A). Livers sections were also extracted and analyzed for the presence of 3OC12-acid. As with the lung tissue, an appreciable amount of 3OC12-acid was detected in the liver tissues (Fig 14B).

One possibility for the lack of PON2 inactivation in vivo after direct perfusion of tissues with 200 µM 3OC12 is that concentrations reached were not high enough to adequately expose cells deep within the tissues, i.e. a high percentage of the cells. As an approach to overcome this we identified a simple method to make micelles containing high concentrations 3OC12(4). We speculated that such high concentrations of 3OC12 in this lipophilic carrier complex may allow a much more extensive exposure of cells within the lungs to the compound. Lungs of deeply anesthetized mice were filled through the trachea with 2 ml of 500 µM of 3OC12 in the micellar solution and left for 1 hour before harvesting. Control mouse lungs received micelles containing the D-3OC12 isomer. The D-3OC12 isomer is not biologically active and we have previously shown that it is not hydrolyzed by PON2(3). Lung sections were weighed and frozen at -80^{o}C until use. Sections were then homogenized and homogenates analyzed for PON2 3OC12 activity. The PON2 activity in the control mice (n=3) was 10.0 ± 1.2 nmol/min/mg of homogenate and the PON2 activity in the L-3OC12 treated mice (n=4) was 10.3 ± 0.3 nmol/min/mg of homogenate. The lack of PON2 inactivation by L-3OC12 suggests that even in the lipophilic micelle carrier complexes 3OC12 still can't disperse to a large enough proportion of lung cells or that many of the types of cells in the mouse lung are resistant to acidification/PON2 inactivation or both.

Lung sections from treated mice were also extracted and analyzed for the presence of 3OC12 by the PDAM/HPLC method. The estimated 3OC12-acid in the lungs of D-3OC12 treated (n=3) and L-3OC12 treated (n=4) mice was 22 ± 12 nmol/g of lung and 362 ± 91 nmol/g of lung. Thus, despite a lack of inactivation of PON2, it is clear that 3OC12 is becoming hydrolyzed and trapped within lung cells.

We hypothesize that the inability of 3OC12 to mediate PON2 inactivation in our in vivo/ex vivo studies is likely due to the lack of exposure of most cells within an organ to sufficient *amounts* of 3OC12 needed to cause adequate intracellular 3OC12-acid accumulation to appreciably decrease the pH. We directly tested this concept in vitro by treating cells with the same *concentration* but different *amounts* of 3OC12. To achieve this, cells were treated with different amounts of 3OC12 by incubating 90,000 cells in different volumes of media containing 100 µM 3OC12. Despite all cells being treated with the same 3OC12 concentration, PON2 was not inactivated when treated with 2 nmols 3OC12 (in 20 µls) but was inactivated by over 50% when treated with 25 nmols (in 250 µls; Fig 15). This illustrates that PON2 inactivation by 3OC12 does not result from a classic ligand-receptor interaction, but that each 3OC12 molecule is essentially "used up" to directly lower the intracellular pH. Unlike a classical ligand-receptor interaction, a single 3OC12 molecule is not available to continually stimulate a cognate receptor or multiple receptors. The implications of this are that cells directly exposed to 3OC12, such as endothelial cells after iv administration of 3OC12 to mice or cells in close proximity to *P. aeruginosa* colonies during infection, will sequester and hydrolyze most of the 3OC12 (resulting in the intracellular accumulation of 3OC12-acid) precluding exposure of underlying cells to significant amounts of 3OC12. Thus, we hypothesize that only the cells immediately exposed to 3OC12 will achieve high enough intracellular 3OC12-acid levels to undergo PON2 inactivation and the other biological effects mediated by acidification. Although it remains possible that a lower specific activity of mouse PON2, compared to human PON2, or lower expression of PON2 in the mouse cells analyzed, may contribute to a higher resistance of PON2 inactivation in the mouse cells. A detailed discussion of this principle and its relevance to *P. aeruginosa* infection can be found in the Discussion section of appendix I.

IV. Key Research Accomplishments

- Demonstrated that 3OC12-acid specifically accumulates within the ER and mitochondria, supporting our hypothesis that acidification within these organelles is the proximal event mediating immediate 3OC12 immunomodulatory bio-effects.
- Demonstrated that intracellular acidification is the proximal event mediating PON2 inactivation.
- Identified prototypical compounds that limit acidification and may be developed as potential drugs to prevent both PON2 inactivation *and* immunomodulatory effects by 3OC12.
- 3OC12-mediated, and PON2-dependent, intracellular acidification mechanism causes immediate bio-effects in primary human bronchial epithelial cells, cells that come into direct contact with *P. aeruginosa* during infection.
- Identified GRP78 as a PON2 interacting protein after 3OC12 treatment of cells.
- Demonstrated that 3OC12-acid accumulates inside mouse lung cells after in vivo treatment with 3OC12.
- Provided evidence that PON2 is inactivated via an ER-stress like mechanism.

V. Conclusions

Our data convincingly demonstrate that PON2-dependent acidification is the proximal event that mediates inactivation of PON2 by 3OC12. Also, we show that cytosolic calcium induction does not mediate PON2 inactivation. The irreversible inactivation of PON2 by 3OC12 does not appear to be a direct result of low pH and calcium driven denaturation or damage to the enzyme (Fig 5). Our finding that thapsigargin, which unlikely results in substantial intracellular acidification, potently inactivates PON2 concurs with a lack of pH driven PON2 denaturation/damage. We identified GRP78 (an ER stress response protein that is a member of the heat shock 70 protein family) as binding to PON2 after 3OC12-mediated inactivation. Thus, based on our current findings, we propose that PON2 is being inactivated by a stress like cellular response that results in the interaction of stress response proteins with PON2. We are continuing to investigate this hypothesis.

Substantial progress has also been made in detailing the novel acidification mechanism by which PON2 mediates immunomodulatory effects of 3OC12. Our data suggests that PON2 is likely a central player in potentiating host cellular responses to 3OC12 that may benefit *P. aeruginosa* virulence. Thus, PON2 may be a double edged sword, simultaneously promoting immunomodulatory effects of 3OC12 (via driving intracellular acidification and disrupting host cell responses) and also protecting against quorum sensing by *P. aeruginosa* via hydrolyzing and inactivating 3OC12. An ideal therapeutic approach would be to prevent the acidification-driven immunomodulatory effects of 3OC12, while simultaneously maintaining the 3OC12-inactivating potential of PON2. We have identified two prototypical compounds, W7 and sphingosine, that can do just that. These weak basic compounds were shown to prevent acidification and PON2 inactivation by 3OC12. Thus, future studies aimed at evaluating this class of compounds as therapeutics to attenuate *P. aeruginosa* pathogenicity is warranted.

Under Aim 2 we were unable to demonstrate PON2 inactivation after 3OC12 administration in vivo to mice. Despite the lack of PON2 inactivation, our data do demonstrate that 3OC12 is undergoing intracellular hydrolysis and accumulation as 3OC12-acid. This provides evidence that PON2-dependent acidification-mediated immunomodulatory effects of 3OC12 are operable in the mice, although additional studies would be necessary to verify this. The reason why we cannot detect PON2 inactivation by 3OC12 in our model in vivo is not clear. We have clearly shown that primary human bronchial epithelial cells are sensitive to PON2 inactivation by 3OC12. Thus, we propose, as discussed above and in the Discussion in appendix I, that the cells in close proximity to bacterial colonies will likely undergo PON2 inactivation in infected subjects. However, we also consider that mouse cells exposed to 3OC12 may be less sensitive to PON2 inactivation that the human bronchial epithelial cells, possibly due to a better ability to maintain proper pH within the ER and mitochondrial compartments. Additionally, we consider that mouse PON2 hydrolyzes 3OC12 with lower efficiency, resulting in less acid accumulation and subsequently less intracellular acidification.

VI. Publications, Abstracts and Presentations

Submission of a full length manuscript entitled, “A novel paraoxonase 2-dependent mechanism mediating the biological effects of a *Pseudomonas aeruginosa* virulence molecule” to The Journal of Biological Chemistry for publication.

VII. References

1. Casey, J. R., Grinstein, S., and Orlowski, J. (2010) Sensors and regulators of intracellular pH. *Nat.Rev.Mol.Cell Biol.* **11**, 50-61
2. Kuo, C. L., and La Du, B. N. (1998) Calcium binding by human and rabbit serum paraoxonases. Structural stability and enzymatic activity. *Drug Metab Dispos.* **26**, 653-660
3. Horke, S., Witte, I., Altenhofer, S., Wilgenbus, P., Goldeck, M., Forstermann, U., Xiao, J., Kramer, G. L., Haines, D. C., Chowdhary, P. K., Haley, R. W., and Teiber, J. F. (2010) Paraoxonase 2 is down-regulated by the Pseudomonas aeruginosa quorumsensing signal N-(3-oxododecanoyl)-L-homoserine lactone and attenuates oxidative stress induced by pyocyanin. *Biochem.J.* **426**, 73-83
4. Valentine, C. D., Zhang, H., Phuan, P. W., Nguyen, J., Verkman, A. S., and Haggie, P. M. (2013) Small molecule screen yields inhibitors of pseudomonas homoserine lactone-induced host responses. *Cell Microbiol.*
5. Brekke,O.L., Sagen,E., & Bjerve,K.S. Tumor necrosis factor-induced release of endogenous fatty acids analyzed by a highly sensitive high-performance liquid chromatography method. *J. Lipid Res.* **38**, 1913-1922 (1997).

VIII. Appendix I

A novel paraoxonase 2-dependent mechanism mediating the biological effects of a *Pseudomonas aeruginosa* virulence molecule[*]

Sven Horke[§¶†], Junhui Xiao[‡†], Eva-Maria Schütz[§], Gerald L. Kramer[‡], Petra Wilgenbus[§], Ines Witte[§], Moritz Selbach[§], Ulrich Förstermann[§] and John F. Teiber[‡1,]

[†]These authors contributed equally to the work

[§]Department of Pharmacology, University Medical Center of the Johannes Gutenberg University Mainz, Obere Zahlbacher Str. 67, 55131 Mainz, Germany

[¶]Center for Thrombosis and Hemostasis, University Medical Center of the Johannes Gutenberg University Mainz, Langenbeck Str. 1, 55131 Mainz, Germany

[‡]Department of Internal Medicine, Division of Epidemiology, The University of Texas Southwestern Medical Center, Dallas, TX 75390, USA

[*]Running Title: *A novel mechanism of P. aeruginosa biological effects*

[1]To whom correspondence should be addressed: John F. Teiber, Department of Internal Medicine, Division of Epidemiology, The University of Texas Southwestern Medical Center, 5323 Harry Hines Blvd., Dallas, TX 75390-8874, USA, Tel.: 214 648 2454; Fax: 214 648 7893; E-mail: john.teiber@utsouthwestern.edu

Keywords: Acyl-homoserine Lactone, Bacterial Pathogenesis, Host Defense, Host-Pathogen Interactions, Innate Immunity, Paraoxonase, *Pseudomonas aeruginosa*, Quorum Sensing

Background: The bacterial signaling molecule 3OC12 elicits many immunomodulatory responses in host cells through uncertain mechanisms.
Results: Human paraoxonase 2 hydrolyzed 3OC12 intracellularly to its hydroxyl acid, resulting in intracellular acidification, calcium release, and kinase activation.
Conclusion: Paraoxonase 2 mediates cellular responses to 3OC12 via a non-receptor mechanism in host cells.
Significance: Elucidation of host-pathogen interactions will help identify novel therapeutic strategies.

ABSTRACT

Pseudomonas aeruginosa **produces *N*-(3-oxo-dodecanoyl)-L-homoserine lactone (3OC12), a crucial signaling molecule that elicits diverse biological responses in host cells thought to subvert immune defenses. The mechanism mediating many of these responses remains unknown. Here we demonstrate in cell lines and in primary human bronchial epithelial cells that 3OC12 is rapidly hydrolyzed intracellularly by the lactonase paraoxonase 2 (PON2) to 3OC12-acid, which becomes trapped and accumulates within the cells. Subcellularly, 3OC12-acid accumulated within the endoplasmic reticulum and mitochondria, compartments where PON2 is localized. Treatment with 3OC12 caused a rapid cytosolic and mitochondrial pH decrease, calcium release and phosphorylation of *stress signaling kinases*. All of these effects were dependent upon PON2 activity. The results indicate a novel, PON2-dependent intracellular acidification mechanism by which 3OC12 can mediate its biological effects.**

Pseudomonas aeruginosa (*PA*) is a common pathogen causing serious infections in immunocompromised and ill individuals due to the bacteria's ability to evade host immune responses and acquire antibiotic resistance(5). Many gram-negative bacteria, including *PA*, produce acyl-homoserine lactone (AHL) signaling molecules which regulate the cell-density-dependent expression of virulence factors in a process termed quorum sensing (QS)(5). The AHL *N*-(3-oxododecanoyl)-L-homoserine lactone

(3OC12) is a key *PA* QS signal that has been shown to be necessary for biofilm maturation and full expression of virulence in *PA* animal infection models(6-9). Concentrations of over 6 μM 3OC12 have been detected in the sputum of individuals with pulmonary *PA* infections(10), suggesting active 3OC12 signaling in the human disease as well. However, concentrations up to 600 μM 3OC12 have been measured in *PA* biofilms in vitro(11). The low μM 3OC12 concentrations detected in the sputum samples are likely to be significantly lower than local concentrations near *PA* colonies due to dilution into a large volume of sputum and enzymatic hydrolysis(10).

In addition to modulating bacterial gene expression, 3OC12 elicits a multitude of biological responses in diverse mammalian cell types(12). Depending upon the cell type 3OC12 induces apoptosis, ER-stress, chemotaxis and pro-inflammatory gene expression (12-14). Conversely, 3OC12 inhibited lipopolysaccharide (LPS) induction of pro-inflammatory mediators in macrophages, fibroblasts, epithelial cells and in vivo by repressing nuclear factor κ-light chain enhancer of activated B-cells (NF-κB) signaling(15). In antigen-stimulated T-lymphocytes, 3OC12 inhibits cell proliferation and production of interferon-γ and IL-4, critical regulators of immunity(12,16). These diverse responses suggest that 3OC12 acts through multiple, and cell type dependent, mechanisms.

Delineating the role of 3OC12 in *PA* pathogenicity is difficult due to the multitude of often disparate effects it has on host cells, but also because the mechanisms by which 3OC12 mediates these effects are poorly understood. 3OC12 does not act through immune pattern recognition receptors such as Toll-like receptors and nucleotide binding, oligomerization domain-like receptors(17). In sinonasal epithelial cells the T2R38 receptor mediated a rapid Ca^{2+} and NO release by 3OC12, however T2R38 likely only mediates responses in upper respiratory cell types(18). Due to its lipophilicity, 3OC12 rapidly enters mammalian cells(16). 3OC12 can interact with nuclear hormone peroxisome proliferator activated receptor (PPAR) transcription factors, resulting in increased cytokine expression(19). However, such effects are relatively slow, occurring at ≥ 6 hours after 3OC12 treatment. Many effects of 3OC12, such Ca^{2+} release and kinase activation, occur within 5 minutes of treatment(3,17,20), a timeline preceding any gene expression. Other mechanisms of 3OC12-mediated effects have been proposed such as disruption of protein interactions and functions through intercalation into plasma membranes or covalent protein modification(21,22). However, evidence for such mechanisms is lacking and the mechanism(s) mediating many cellular responses to 3OC12 remains unknown.

The paraoxonase (PON) family of mammalian esterases, PON1, PON2 and PON3 hydrolyze AHLs to their ring-opened biologically inactive carboxylic acid counterparts(23). PON2 is expressed intracellularly, is widely found in mammalian tissues and cell types and very efficiently hydrolyzes 3OC12 to 3OC12-acid (23-28). Independent of its hydrolytic activity, PON2 also has antioxidant activity and can protect cells from endoplasmic reticulum (ER) stress, including ER stress induced by 3OC12(25,26,29). Such findings suggest that PON2 may be an important component of the innate defense by interfering with bacterial QS and attenuating 3OC12-mediated effects on host cells.

Here we identify a unique mechanism by which PON2 also mediates biological effects of 3OC12. We demonstrate that PON2 catalyzes the rapid hydrolysis of 3OC12 to 3OC12-acid, resulting in intracellular accumulation of 3OC12-acid, cytosolic acidification, calcium release and phosphorylation of p38 and eIF2-α. Thus, PON2 may be a double edged sword, disrupting bacterial QS and protecting from ER stress while simultaneously promoting immunomodulatory effects of 3OC12 in host cells.

EXPERIMENTAL PROCEDURES

Cells - Generation and culturing of stable PON2 / PON2-H114Q overexpressing EA.hy 926 (EA.hy) cells and PON2 overexpressing HEK cells has been described(25,30). Primary human bronchial epithelial cells (HBEC), human umbilical vein endothelial cells (HUVEC) and primary cell media and supplement mixes were from PromoCell and cells were cultured as recommended by the supplier.

PON2 activity - PON2 3OC12 (Sigma Aldrich) hydrolytic activity was determined by HPLC as previously described(23). Activity is expressed as units per mg of lysate or purified protein. One unit

equals 1 nmol of 3OC12 hydrolyzed per min. Recombinant human PON2 was purified as previously described(31).

Intracellular 3OC12-acid determination - Cells were seeded in 24 well plates, and the following day (at approximately 75% confluence) treated with 0.5 ml of media containing 3OC12 and placed back in the cell culture incubator. At given times the cells were rinsed with PBS and extracted with 100 µl cold acetonitrile containing 25 µM *N*-dodecanoyl-L-homoserine lactone as the internal standard. Extracts were centrifuged for 1 min at 14,000 x *g* and analyzed by HPLC as previously described(23). The concentration of 3OC12-acid in each sample was calculated from peak areas using a standard curve generated from 3OC12-acid standards. The 3OC12-acid was prepared by incubating 3OC12 in 5 mM NaOH for 2 hrs. Complete hydrolysis of 3OC12 to the 3OC12-acid was confirmed by HPLC analysis. Protein concentrations of cells were determined by lysing in RIPA buffer, sonicating and analyzing lysates using the BCA method (Thermo Scientific).

For determination of 3OC12-acid accumulation within the ER and mitochondria, 5 x 10^6 cells were suspended in 10 ml media without or with 50 µM 3OC12 for 30 min at 37^{o}C. The cells were isolated and washed with PBS. Mitochondria were isolated as previously described(29), except that following the 10,000 x g spin the mitochondrial pellet was washed with mitochondrial buffer, transferred to a new 1.5 ml Eppendorf tube and re-centrifuged at 10,000 x g. Microsomes were isolated as previously described with minor modifications(32). Briefly, cells were in dounce homogenized in 0.75 ml of TBS containing 1 mM EDTA and 0.8 M sucrose. Aliquots (180 µls) were placed in 1.5 ml tubes and centrifuged at 600 x g for 10 min. The supernatants were carefully removed, diluted 1:1 in water and centrifuged at 21,000 x g for 40 min to obtain microsomal pellets. The microsomal and mitochondrial pellets were extracted with 50 µl acetonitrile containing 0.4 % dodecylmaltoside (Dojindo) and analyzed 3OC12-acid by HPLC as described above. To control for any 3OC12-acid potentially precipitating out of solution and/or associating with the mitochondria or microsomes in a non-specific manner, additional controls were analyzed in which 50 µM 3OC12-acid was added to the cell homogenate from untreated cells, followed by isolation of organelles. In these controls a small amount of 3OC12-acid was associated with the microsomal and mitochondrial pellets. This background level of 3OC12-acid was subtracted from 3OC12-acid measured in the pellets isolated from 3OC12 treated cells. The microsomal and mitochondrial protein, precipitated after acetonitrile extraction, was dissolved in 1 M NaOH overnight and quantified with the BCA method.

Cytosolic pH and Ca^{2+} measurements - For determination of pHi and $[Ca^{2+}]_c$ cells were seeded in black 96-well Costar plates so that they were 80-90% confluent at the time of assay. Treatments were performed at 37°C. For pHi determination, cells were loaded with 2 µM BCECF-AM (Invitrogen) in 100 µl of media for 40 min, washed and incubated for 15 min with Hank's balanced salt solution containing Ca^{2+} and Mg^{2+} (HBSS). Cells were washed again, treated with 3OC12 with or without triazolo[4,3-*a*]quinolone (TQ416; ChemDiv) or an equivalent volume of DMSO as the control, in 100 µl of HBSS and fluorescence was measured using a Synergy HT fluorometric plate reader (Bio-Tek) with excitation wavelengths set at 485 nm and 360 nm and emission detected at 528 nm. The calibration of pHi was performed on cells using high KCl buffers containing nigericin as previously described(33).

Intracellular Ca^{2+} was determined as previously described with minor modifications(25). Plated cells were loaded with 4 µM Fluo-4 AM (Invitrogen) in medium containing 20 mM Hepes and 2.5 mM probenicid for 45 min and then washed 3 times in HBSS. Cells were treated with HBSS containing DMSO (controls), 3OC12 or m-3M3FBS (EMD Millipore) and fluorescence was measured for 25 min with excitation and emission wavelengths of 480 nm and 530 nm, respectively.

Confocal microscopy - EA.hy cells were seeded at 1 x 10^4 in 4-well slide cover glass-I chambers (Greiner Bio-One). The next day, cells were loaded with SNARF-4F and Fluo4-AM (5 and 1 µM, respectively; Invitrogen) in Krebs buffer (Noxygen) at 37°C for 1 h. After brief washes, chambers were loaded on a 37°C / 5% CO_2 incubator device mounted on a confocal Zeiss LSM710 laser-scanning microscope. Upon

exposure to 3OC12, cells were immediately imaged with a EC Plan-Neofluar 20x/0.50M27 objective, 4.07 µsec pixel dwell, 54 µm pinhole and emission wavelengths of 493-516 nm (Fluo-4AM); SNARF-4F was calculated as ratio of acidic (581-601 nm) / basic (650-738 nm) fluorescence units. Thus, increased ratio indicates acidification. Using ZEN2009 software (Zeiss), the fluorescence intensities at every time point were recorded for approximately 50-100 cells per visible field and transferred to GraphPad prism software (GraphPad Software Inc.) for evaluation and data processing.

Mitochondrial pH $[pH]_m$ was determined as follows: HEK or EA.hy 926 cells were seeded in LabTek chambers (1.3×10^5 / chamber with 4 chambers per slide; Sarstedt). The next day, cells were gently washed with HBSS, stained with SNARF-1-AM (5 µM; Invitrogen) in HBSS for 10 min at 37°C and then kept in MICA buffer (145 mM KCl, 1.5 mM $CaCl_2$, 1 mM $MgSO_4$, 10 mM HEPES, 5.5 mM glucose, adjusted to pH 7.5 with Tris) for 3 h to allow mitochondrial targeting of SNARF-1. During a further 15 min incubation time with DiOC6 (5 nM; Invitrogen; in HBSS) to co-stain mitochondria, chambers were mounted on the microscope for imaging. Cells were then treated with 50 µM 3OC12 in 500 µl of MICA buffer per chamber, accompanied by imaging on a Zeiss LSM 710 (Plan/Apochromat x 63/1.4 oil DIC objective; 1 min intervals for 15 min; Z-stacking with 5-8 levels per image at 1 AU; excitation at 488 and 543 nm; emission at 500-520 nm for DiOC6 / 580-595 nm for acidic SNARF-1 / 650-730 nm for basic SNARF-1). ImageJ software was used to evaluate SNARF-1 ratiometric changes in all single Z-stacks for any time-point using DiOC6 staining as mitochondrial mask in order to only collect mitochondrial SNARF-1 signals. Changes in $[pH]_m$ were calculated after preceding calibration with 10 µM nigericin-containing MICA buffers covering a pH range from 6.8 to 8.1. EA.hy 926 cells differed in that SNARF-1 incubation time was 90 min, which resulted in near complete overlap of SNARF-1 fluorescence with that of mitochondrial DiOC6.

Western blotting - All lysates were produced in the presence of PhosphoStop phosphatase inhibitor (Roche) and HALT protease inhibitor (Thermo Scientific). The PON2 antibody and immunoblotting has been previously described(25). Antibodies against eIF2α / phospho-eIF2a (Ser51) and p38 (Thr180/Tyr182) were from Cell Signaling and used as recommended. Anti-GAPDH (clone 6C5; Santa Cruz) and mouse-anti-Tubulin Ab2 (Dianova) were used at 1:5000. HRP-conjugated secondary antibodies were from Cell Signaling.

RNA interference - Approximately 60% confluent cells were transfected with 50 nM PON2-specific or scrambled Stealth siRNA (Invitrogen) using either SaintRed (Synvolux) or Lipofectamine RNAiMax (Invitrogen) transfection reagent according to the suppliers instructions. siRNA sequences and methods have been previously described(34). Stimulation with 3OC12 or LPS (*Escherichia coli* 0111:B4; Sigma) was performed 2.5 – 3 days after treatment, since this was the time point of maximal knock-down. Efficiency was about 50-60% in HUVEC and ≥ 80% in all other cells (at protein and activity levels). Levels of phospho-p38 or phospho-eIF2a were normalized to total p38 or eIF2a levels, respectively.

Statistical analysis - Curve fitting and statistical analysis were performed with GraphPad Prism software.

RESULTS

PON2 mediates intracellular 3OC12-acid accumulation - We and others had previously observed that 3OC12-acid accumulated inside cells after treatment with 3OC12(17). This suggested that the hydrophobic 3OC12 is hydrolyzed inside the cell to its corresponding ring-opened 3OC12-acid, which is much more polar and likely unable to readily cross cellular membranes. We therefore measured the rates of intracellular accumulation of 3OC12-acid in human embryonic kidney cells (HEK) and HEK PON2 cells stably transfected with a human PON2-GFP construct. The HEK cells express low basal levels of PON2, 2.2 ± 0.2 U/mg, while the stably transfected HEK PON2 cells have 70.4 ± 7.0 U/mg of PON2. When treated with 3OC12, the rate of intracellular 3OC12-acid accumulation was much faster in the HEK PON2 cells and began to plateau rapidly, within 4 min (Fig 1A). The plateau could at least partly be due to the resulting acidification which would decrease the

rate of pH-dependent lactone hydrolysis and the ability of 3OC12 to cause inactivation of PON2 activity(3,35).

We also compared the rates of intracellular accumulation of 3OC12-acid in a human endothelial cell line EA.hy 926 stably transfected with human PON2 (EA.hy PON2) or an inactive PON2 H114Q mutant (EA.hy H114Q). The PON2 mutant retains its antioxidant and antiapoptotic functions, but does not have 3OC12 hydrolytic activity(34). Thus, this PON2 mutant controls for effects due to increased protein expression and any effects of PON2 not associated with its hydrolytic activity. We have also previously established that PON2 is the only enzyme that hydrolyzes 3OC12 in EA.hy cells(23). The EA.hy H114Q cells have 6.8 ± 0.4 U/mg of PON2 activity, due to significant basal levels of PON2, while the EA.hy PON2 cells have 25.8 ± 2.5 U/mg of PON2 activity. The rate of accumulation of 3OC12-acid in the EA.hy PON2 cells was significantly faster compared to the EA.hy H114Q cells and also began to plateau rapidly (Fig 1B).

The contribution of PON2 to 3OC12-acid accumulation was also evaluated in primary human bronchial epithelial cells (HBEC), cells that come into direct contact with *PA* during pulmonary infections. The cells were first transfected for 3 days with PON2 siRNA, to decrease PON2 levels, or scrambled siRNA as controls. Upon treatment with 3OC12, 3OC12-acid accumulated rapidly in the HBEC and this accumulation was significantly diminished in the PON2 siRNA treated cells (Fig 1C). 3OC12 was not detected in any of the cells at any time point (detection limit 0.5 nmol/mg of cell lysate). These results demonstrate that rapid intracellular accumulation 3OC12-acid largely depends on hydrolytically active PON2.

3OC12 causes a rapid PON2-dependent cytosolic acidification and calcium release - The rapid intracellular accumulation of 3OC12-acid suggested a potential corresponding decrease in intracellular pH (pHi). Therefore, we directly visualized the change in pHi in naïve (non-transfected) EA.hy cells after 3OC12 treatment by laser scanning confocal microscopy. Because decreased pHi can induce Ca^{2+} release and increased cytosolic Ca^{2+} $[Ca^{2+}]_c$ is a common response to 3OC12 in mammalian cells(12,36), we also concomitantly measured $[Ca^{2+}]_c$ fluxes. The cells were simultaneously loaded with the Ca^{2+} indicator Fluo-4 AM and the pH indicator SNARF-4F, treated with 3OC12, and time lapse images acquired. As shown in figure 2A and B, 3OC12 caused a very rapid decrease in cytosolic pHi (as measured by an increase in SNARF-4F fluorescence) and increase in $[Ca^{2+}]_c$. Interestingly, the rapid pHi decrease appeared to return to initial levels within 4 min, but then decreased again before slowly returning to initial levels (Fig 2B). The decrease in pHi appeared to just precede the increase in $[Ca^{2+}]_c$, consistent with a potential intracellular acidification mediating Ca^{2+} release into the cytosol.

The ability of 3OC12 to cause cytosolic acidification and calcium release was also evaluated with the pH indicator BCECF-AM and Fluo-4 AM, respectively, in the HBEC. 3OC12 caused a rapid and dose-dependent pHi decrease and $[Ca^{2+}]_c$ increase (Fig 2C and D). The pHi began to recover after 30 min (Fig 2C), but at slower rate than in the EA.hy cells. The $[Ca^{2+}]_c$ remained elevated in the HBEC even after 25 min (2D). Thus, different cell types react with individual kinetics, however the general responses to 3OC12 are consistent.

The role of PON2 in the 3OC12-mediated pHi and $[Ca^{2+}]_c$ changes was evaluated in the PON2-expressing cell lines as well as in the HBEC transfected with PON2 siRNA. In the HEK cells 3OC12 caused no detectable change in pHi and a slow, minor rise in $[Ca^{2+}]_c$ (Fig 3A and D). Conversely, in the HEK PON2 cells 3OC12 caused a rapid, almost immediate, decrease in pHi with a concomitant pronounced rise in $[Ca^{2+}]_c$ (Fig 3A and D). Unlike in the HBEC, the pHi and $[Ca^{2+}]_c$ returned to initial levels relatively quickly, by 10-15 min post treatment. 3OC12 also caused rapid decrease in pHi with a concomitant increase in $[Ca^{2+}]_c$ in the EA.hy H114Q and EA.hy PON2 cells (Fig 3B and E). However, compared to the EA.hy H114Q cells, the pHi decrease and the $[Ca^{2+}]_c$ increase in the EA.hy PON2 cells were significantly greater. Also, the increase in $[Ca^{2+}]_c$ was delayed in the EA.hy H114Q cells compared to the EA.hy PON2 cells. Within each cell type the extent of intracellular acidification and $[Ca^{2+}]_c$ flux corresponded closely with the time course of 3OC12-acid accumulation and cellular PON2 levels. The pHi and $[Ca^{2+}]_c$ changes in the EA.hy

H114Q and EA.hy PON2 cells were also transient, lasting 20-25 min.

Lowering PON2 levels by RNAi in the HBEC nearly eliminated the 3OC12-mediated acidification and $[Ca^{2+}]_c$ rise (Fig. 3C and F). PON2 had no direct effect on calcium release as treatment of HBEC with the phospholipase C activator m-3M3FBS, which generates inositol phosphate and subsequent release of intracellular calcium stores, resulted in the same $[Ca^{2+}]_c$ increases in both the PON2 and scrambled siRNA transfected cells (Fig. 3F). Thus, as with the cell lines, the 3OC12-mediated pHi and $[Ca^{2+}]_c$ changes are dependent upon PON2 in the primary HBEC.

3OC12 causes a PON2-dependent phosphorylation of MAPK p38 and eIF2α - p38 and eIF2α are kinases that are activated in response to stressors. Activated eIF2α inhibits protein translation and is a marker of ER stress, and phosphorylation of both p38 and eIF2α are established immediate responses to 3OC12((15) and Fig. 4A). Furthermore, p38 is phosphorylated in response to intracellular acidification(37). Therefore, we hypothesized the phosphorylation of these kinases by 3OC12 treatment would be dependent on PON2. Compared to naïve EA.hy cells and EA.hy H114Q cells the EA.hy PON2 cells exhibited increased p38 and eIF2α phosphorylation in response to 3OC12 (Fig. 4B-D). Phosphorylation of p38 by LPS was the same in the EA.hy naïve, H114Q and PON2 cells demonstrating that PON2 only affects 3OC12-mediated p38 phosphorylation (Fig. 4B-D).

To see if such effects were also dependent on PON2 in primary cells, phosphorylation of p38 and eIF2α was investigated in both primary human umbilical vein endothelial cells (HUVECs) and the HBEC. Decreasing PON2 levels by RNAi also diminished the 3OC12-mediated p38 and eIF2α phosphorylation in the HUVECs (Fig 4E and F). Treatment of HBEC with 25 μM 3OC12 for 10 min did not induce p38 or eIF2α phosphorylation (Fig 4G-H). p38 and eIF2α phosphorylation was induced by treating HBECs with 50 μM 3OC12 for 10 min and by 25 μM and 50 μM 3OC12 for 30 min (Fig 4G-H). In all treatments that induced p38 and eIF2α phosphorylation, decreasing PON2 levels by RNAi significantly diminished phosphorylation (Fig 4G-H). Collectively, the data demonstrate the 3OC12-mediated phosphorylation of p38 and eIF2α are dependent upon PON2.

3OC12-acid accumulates within the ER and mitochondria - PON2 is predominantly localized to the inner mitochondrial membrane and likely facing the lumen in the ER(29,38,39). Therefore, we hypothesized that (i) it is within these organelles where 3OC12-acid is predominantly accumulating and (ii) the pH drop measured in the cytosol is a reflection of a much greater pH drop within the ER and/or mitochondria. HEK PON2 cells were treated for 30 min with 50 μM 3OC12 and microsomes and mitochondria were isolated, extracted and the extracts analyzed for 3OC12-acid. 3OC12-acid was present inside the microsomes and mitochondria at 12.7 ± 1.9 and 3.9 ± 0.6 nmol/mg protein, respectively. The isolated microsomal and mitochondrial pellets were very small; occupying less than 0.5 μl in volume. Thus, the concentration of 3OC12-acid inside the microsomes and mitochondria can be estimated at greater than 324 μM and 220 μM, respectively, or 4-6 fold greater than the concentration of 3OC12 the cells were treated with. No 3OC12 was detected in the microsomes or the mitochondria.

We then determined if 3OC12 could decrease pH specifically within the mitochondria. EA.hy 926 cells stably overexpressing non-fluorescent PON2-HA or the empty plasmid (pCDNA3-HA;(25)) were loaded with SNARF-1, a ratiometric pH indicator targeting the mitochondria. $[pH]_m$ was visualized by 3D multicolor time-lapse live cell imaging. To account for mitochondrial movement and cell morphology changes during imaging, tracking of mitochondria through different image layers was established by concomitant cell loading with the mitochondrial dye DiOC6. The low concentration of DiOC6 (5 nM) did not stain ER membranes and perfectly merged with dyes such as MitoTracker-Orange (not shown). Using the DiOC6 signal as mask, SNARF1 ratios at DiOC6-positive areas, i.e. mitochondria, were quantified. This enabled estimation of SNARF1 ratios for all recorded Z-layers at every time point. A calibration curve had been established by nigericin-containing buffers at different pH values. As shown in Fig. 5A and B, 3OC12 treatment of control EA.hy 926 resulted in an immediate decrease of $[pH]_m$ during the first 10

min. Upon overexpression of PON2, this acidification was enhanced (Fig. 5B). Mitochondrial acidification in response to 3OC12 was also seen in HUVECs and, to a lower extent, in HEK cells (not shown). Collectively, these data imply a general mitochondrial acidification in response to 3OC12 exposure dependent on PON2.

A small molecule inhibitor of 3OC12-mediated cellular responses also inhibits PON2 – The triazolo[4,3-*a*]quinolone compound TQ416 was recently identified in a high throughput screen as a potent inhibitor of 3OC12 effects in cell cultures(4). At a concentration of 1 μM, TQ416 restored the 3OC12-mediated inhibition of LPS induced NF- κB activation and prevented 3OC12-induced $[Ca^{2+}]_c$ release, phosphorylation of p38, and caspase activation(4). This suggested to us that TQ416 may be preventing these effects of 3OC12 via inhibiting PON2 activity. Indeed, TQ416 was a potent inhibitor of PON2 3OC12 hydrolysis (Fig 6A). TQ416 also potently inhibited 3OC12-mediated cytosolic acidification in EA.hy PON2 cells (Fig. 6B). These findings suggest that at least some of the inhibitory effects of TQ416 on 3OC12's biological actions are via inhibition of PON2-dependent 3OC12 intracellular acidification.

DISCUSSION

3OC12 elicits a spectrum of biological effects in diverse host cell types, many of which are believed to favor *PA* persistence. While 3OC12 can activate the T2R38 receptor in sinonasal cells, and modulate PPAR receptor activities, the mechanism mediating many of 3OC12's effects remains enigmatic(18,19). Here we demonstrate in both cell lines and primary HBECs that $[Ca^{2+}]_c$ increase and phosphorylation of p38 and eIF2-α, common immediate effects of 3OC12, are dependent upon intracellular PON2-mediated hydrolysis of 3OC12 to 3OC12-acid. The time course of 3OC12-acid accumulation corresponds closely with the time course of cytosolic acidification and the measured biological responses. Thus, our data demonstrate a novel mechanism in which PON2 hydrolyzes 3OC12 to its carboxylic acid, which becomes trapped within the cell, causing an intracellular acidification triggering pH-dependent biological responses.

We propose that intracellular acidification is the initial event mediating our observed biological responses to 3OC12. Phosphorylation of p38 by 3OC12, demonstrated to be dependent on PON2 in this study, is known to be induced by intracellular acidification(37). Many proteins that have critical roles in biological functions are very sensitive to minute changes in pH(1). Therefore, cells stringently regulate pHi by employing diverse families of proton extruders and pumps and a balance of intracellular weak acids and bases to increase buffering capacity(1). This propensity of cells to maintain pH homeostasis is exemplified in our cell lines, where cytosolic pHi decreases return to initial levels within 10-20 min after 3OC12 treatment (Fig. 1E and F).

As PON2 is localized to the mitochondria and ER, we hypothesized that 3OC12-acid accumulation and acidification would be predominantly occurring in these organelles. Indeed we demonstrate that 3OC12-acid is concentrating in both the ER and mitochondria and that mitochondria undergo a rapid PON2-dependent acidification after 3OC12 treatment. Mitochondria rely on a proton gradient to drive ATP synthesis and to transport metabolites and ions across that inner mitochondrial membrane, making this organelle exquisitely sensitive to pH changes(40). Thus, we hypothesize that acidification within the mitochondria and possibly the ER is the primary event triggering the pH-dependent biological responses to 3OC12.

Because PON2 is widely expressed in cells and tissues(24,28), most mammalian cells would be expected to hydrolyze 3OC12 intracellularly and potentially undergo subsequent acidification. However, due to the array of pH regulating mechanisms within cells the response of different cell types to 3OC12-acid accumulation would not be expected to be the same(1,37). We found that the rate of intracellular 3OC12-acid accumulation in the HEK PON2 cells was slightly greater than that in the EA.hy PON2 cells, yet the pHi drop was less extensive and had a shorter time course (Figs 1 and 3). Interestingly, despite the less extensive pHi drop in the HEK PON2 cells, the maximal increase in $[Ca^{2+}]_c$ was greater and occurred earlier compared to the EA.hy PON2 cells (Fig 3). Thus, compared to the EA.hy PON2 cells the HEK PON2 cells appear to be more resistant to cytosolic pHi changes, but more sensitive to pHi-mediated $[Ca^{2+}]_c$ induction.

Our findings suggest that, in addition to cellular PON2 levels, the ability of a cell type to regulate pHi and the sensitivity of its signaling pathways to pHi changes will likely be critical factors modulating the response to 3OC12.

The 3OC12 effects reported here occurred at 30 min or less. Exposure to 3OC12 for longer times, ≥4 h, has previously been shown to induce cytokine expression via binding to PPAR receptors(19). 3OC12 treatment of cells for ≥1.5 h was also shown to induce ER stress, which was attenuated by PON2(26,27). The mechanism(s) by which 3OC12 induces ER stress is unknown. However, the findings suggest that 3OC12 may mediate cellular responses through multiple receptor mediated mechanisms (such as nuclear transcription factors or transmembrane receptors) as well as PON2-dependent acidification. For acidification dependent effects, sufficient levels of intracellular 3OC12-acid must be reached to trigger pH-mediated effects. Receptor mediated effects may be more sensitive than the pH-mediated effects. Thus, it's possible that at lower 3OC12 concentrations/levels, receptor mediated effects predominate and PON2 may prevent such effects by inactivating 3OC12 and by limiting oxidative stress. At higher 3OC12 levels, PON2 may induce pH-mediated effects. Whether PON2 prevents or initiates 3OC12 effects may depend upon a multitude of factors including cell phenotype and 3OC12 exposure levels and duration.

The concentration range of 3OC12 used in this study, 25-50 μM, is that which is typically used to evaluate 3OC12's biological effects. However, the levels of 3OC12 that cells are exposed to in vivo during *PA* infection is uncertain and a matter of debate. While concentrations of 3OC12 from 1-10 μM have been measured in planktonic cultures, concentrations of ~ 600 μM have been measured in *PA* biofilms grown in vitro(11). Concentrations of up to 6.9 μM were recently measured in sputum samples from subjects with pulmonary *PA* infections(10). However, the authors of this study indicated that 3OC12 concentrations may be higher near sites of *PA* colonization due to differing environments within the lung and colonization densities. Our findings have significant implications with respect to quantifying the level of 3OC12 produced in vivo. 3OC12 has a very high partitioning coefficient of ~1000:1 in a lipophilic/aqueous system(11). Thus, consistent with our data and that of others(16), 3OC12 produced would be expected to rapidly partition into host cells. Once in the cells, it will be rapidly hydrolyzed by PON2 to 3OC12-acid and become trapped, precluding detection of the metabolite extracellularly. Furthermore, *PA* produces N-acylases with high activity towards 3OC12 that will likely contribute to 3OC12 elimination(41). Therefore, due to intracellular sequestration and hydrolysis, metabolism via bacterial enzymes and dilution into large sputum volumes, the low μM concentrations of 3OC12 measured in sputum samples from infected subjects are likely a significant underestimation of concentrations to which host cells are exposed. The rapid partitioning of 3OC12 into host cells and intracellular entrapment of 3OC12-acid must be considered in future studies designed to determine the amount of 3OC12 produced in vivo during infection.

In summary, this study demonstrates a novel PON2-dependent mechanism by which 3OC12 elicits biological effects in mammalian cells. Additionally, we show that this mechanism is operative in primary human epithelial cells, suggesting that it's biologically relevant. The PON2-mediated intracellular acidification occurs rapidly, and thus likely contributes to many of the previously reported, yet unexplained immediate cellular responses to 3OC12. This finding should greatly accelerate the understanding of how *PA*, as well as other gram-negative bacteria, utilize AHLs to modulate host immune responses. In addition it may reveal novel therapeutic targets which may be exploited to limit the pathogenicity of *PA*.

ACKNOWLEDGEMENTS

J.F.T and S.H. were funded by a U.S. Department of Defense award (W81XWH-12-2-0091). S.H. was also funded by intramural funds from the University Medical Center Mainz, the German Research Foundation (DO1289/6-1), Gerhard and Martha Röttger foundation and the Center for Thrombosis and Hemostasis, Mainz (BMBF funding allocation ID 01E01003, project TRPA1.

REFERENCES

1. Casey, J. R., Grinstein, S., and Orlowski, J. (2010) Sensors and regulators of intracellular pH. *Nat.Rev.Mol.Cell Biol.* **11**, 50-61
2. Kuo, C. L., and La Du, B. N. (1998) Calcium binding by human and rabbit serum paraoxonases. Structural stability and enzymatic activity. *Drug Metab Dispos.* **26**, 653-660
3. Horke, S., Witte, I., Altenhofer, S., Wilgenbus, P., Goldeck, M., Forstermann, U., Xiao, J., Kramer, G. L., Haines, D. C., Chowdhary, P. K., Haley, R. W., and Teiber, J. F. (2010) Paraoxonase 2 is down-regulated by the Pseudomonas aeruginosa quorumsensing signal N-(3-oxododecanoyl)-L-homoserine lactone and attenuates oxidative stress induced by pyocyanin. *Biochem.J.* **426**, 73-83
4. Valentine, C. D., Zhang, H., Phuan, P. W., Nguyen, J., Verkman, A. S., and Haggie, P. M. (2013) Small molecule screen yields inhibitors of pseudomonas homoserine lactone-induced host responses. *Cell Microbiol.*
5. Schuster, M., and Greenberg, E. P. (2006) A network of networks: quorum-sensing gene regulation in Pseudomonas aeruginosa. *Int.J.Med.Microbiol.* **296**, 73-81
6. Hoffmann, N., Rasmussen, T. B., Jensen, P. O., Stub, C., Hentzer, M., Molin, S., Ciofu, O., Givskov, M., Johansen, H. K., and Hoiby, N. (2005) Novel mouse model of chronic Pseudomonas aeruginosa lung infection mimicking cystic fibrosis. *Infect.Immun.* **73**, 2504-2514
7. Nakagami, G., Morohoshi, T., Ikeda, T., Ohta, Y., Sagara, H., Huang, L., Nagase, T., Sugama, J., and Sanada, H. (2011) Contribution of quorum sensing to the virulence of Pseudomonas aeruginosa in pressure ulcer infection in rats. *Wound.Repair Regen.* **19**, 214-222
8. Christensen, L. D., Moser, C., Jensen, P. O., Rasmussen, T. B., Christophersen, L., Kjelleberg, S., Kumar, N., Hoiby, N., Givskov, M., and Bjarnsholt, T. (2007) Impact of Pseudomonas aeruginosa quorum sensing on biofilm persistence in an in vivo intraperitoneal foreign-body infection model. *Microbiology* **153**, 2312-2320
9. Wu, H., Song, Z., Hentzer, M., Andersen, J. B., Molin, S., Givskov, M., and Hoiby, N. (2004) Synthetic furanones inhibit quorum-sensing and enhance bacterial clearance in Pseudomonas aeruginosa lung infection in mice. *J.Antimicrob.Chemother.* **53**, 1054-1061
10. Struss, A. K., Nunes, A., Waalen, J., Lowery, C. A., Pullanikat, P., Denery, J. R., Conrad, D. J., Kaufmann, G. F., and Janda, K. D. (2013) Toward implementation of quorum sensing autoinducers as biomarkers for infectious disease states. *Anal.Chem.* **85**, 3355-3362
11. Charlton, T. S., de, N. R., Netting, A., Kumar, N., Hentzer, M., Givskov, M., and Kjelleberg, S. (2000) A novel and sensitive method for the quantification of N-3-oxoacyl homoserine lactones using gas chromatography-mass spectrometry: application to a model bacterial biofilm. *Environ.Microbiol.* **2**, 530-541
12. Teplitski, M., Mathesius, U., and Rumbaugh, K. P. (2011) Perception and degradation of N-acyl homoserine lactone quorum sensing signals by mammalian and plant cells. *Chem.Rev.* **111**, 100-116
13. Zimmermann, S., Wagner, C., Muller, W., Brenner-Weiss, G., Hug, F., Prior, B., Obst, U., and Hansch, G. M. (2006) Induction of neutrophil chemotaxis by the quorum-sensing molecule N-(3-oxododecanoyl)-L-homoserine lactone. *Infection and Immunity* **74**, 5687-5692
14. Tateda, K., Ishii, Y., Horikawa, M., Matsumoto, T., Miyairi, S., Pechere, J. C., Standiford, T. J., Ishiguro, M., and Yamaguchi, K. (2003) The Pseudomonas aeruginosa autoinducer N-3-oxododecanoyl homoserine lactone accelerates apoptosis in macrophages and neutrophils. *Infect.Immun.* **71**, 5785-5793
15. Kravchenko, V. V., Kaufmann, G. F., Mathison, J. C., Scott, D. A., Katz, A. Z., Grauer, D. C., Lehmann, M., Meijler, M. M., Janda, K. D., and Ulevitch, R. J. (2008) Modulation of gene expression via disruption of NF-kappaB signaling by a bacterial small molecule. *Science* **321**, 259-263
16. Ritchie, A. J., Whittall, C., Lazenby, J. J., Chhabra, S. R., Pritchard, D. I., and Cooley, M. A. (2007) The immunomodulatory Pseudomonas aeruginosa signalling molecule N-(3-oxododecanoyl)-L-homoserine lactone enters mammalian cells in an unregulated fashion. *Immunol.Cell Biol.* **85**, 596-602
17. Kravchenko, V. V., Kaufmann, G. F., Mathison, J. C., Scott, D. A., Katz, A. Z., Wood, M. R., Brogan, A. P., Lehmann, M., Mee, J. M., Iwata, K., Pan, Q., Fearns, C., Knaus, U. G., Meijler, M. M., Janda, K. D., and Ulevitch, R. J. (2006) N-(3-oxo-acyl)homoserine lactones signal cell activation through a mechanism distinct from the canonical pathogen-associated molecular pattern recognition receptor pathways. *J.Biol.Chem.* **281**, 28822-28830
18. Lee, R. J., Xiong, G., Kofonow, J. M., Chen, B., Lysenko, A., Jiang, P., Abraham, V., Doghramji, L., Adappa, N. D., Palmer, J. N., Kennedy, D. W., Beauchamp, G. K., Doulias, P. T., Ischiropoulos, H., Kreindler, J. L., Reed, D. R., and

Cohen, N. A. (2012) T2R38 taste receptor polymorphisms underlie susceptibility to upper respiratory infection. *J.Clin.Invest* **122**, 4145-4159

19. Jahoor, A., Patel, R., Bryan, A., Do, C., Krier, J., Watters, C., Wahli, W., Li, G., Williams, S. C., and Rumbaugh, K. P. (2008) Peroxisome proliferator-activated receptors mediate host cell proinflammatory responses to Pseudomonas aeruginosa autoinducer. *J.Bacteriol.* **190**, 4408-4415
20. Shiner, E. K., Terentyev, D., Bryan, A., Sennoune, S., Martinez-Zaguilan, R., Li, G., Gyorke, S., Williams, S. C., and Rumbaugh, K. P. (2006) Pseudomonas aeruginosa autoinducer modulates host cell responses through calcium signalling. *Cell Microbiol.* **8**, 1601-1610
21. Davis, B. M., Jensen, R., Williams, P., and O'Shea, P. (2010) The interaction of N-acylhomoserine lactone quorum sensing signaling molecules with biological membranes: implications for inter-kingdom signaling. *PLoS.One.* **5**, e13522
22. Garner, A. L., Yu, J., Struss, A. K., Kaufmann, G. F., Kravchenko, V. V., and Janda, K. D. (2013) Immunomodulation and the quorum sensing molecule 3-oxo-C12-homoserine lactone: the importance of chemical scaffolding for probe development. *Chem.Commun.(Camb.)* **49**, 1515-1517
23. Teiber, J. F., Horke, S., Haines, D. C., Chowdhary, P. K., Xiao, J., Kramer, G. L., Haley, R. W., and Draganov, D. I. (2008) Dominant role of paraoxonases in inactivation of the Pseudomonas aeruginosa quorum-sensing signal N-(3-oxododecanoyl)-L-homoserine lactone. *Infect.Immun.* **76**, 2512-2519
24. Mackness, B., Beltran-Debon, R., Aragones, G., Joven, J., Camps, J., and Mackness, M. (2010) Human tissue distribution of paraoxonases 1 and 2 mRNA. *IUBMB.Life* **62**, 480-482
25. Horke, S., Witte, I., Wilgenbus, P., Kruger, M., Strand, D., and Forstermann, U. (2007) Paraoxonase-2 reduces oxidative stress in vascular cells and decreases endoplasmic reticulum stress-induced caspase activation. *Circulation* **115**, 2055-2064
26. Kim, J. B., Xia, Y. R., Romanoski, C. E., Lee, S., Meng, Y., Shi, Y. S., Bourquard, N., Gong, K. W., Port, Z., Grijalva, V., Reddy, S. T., Berliner, J. A., Lusis, A. J., and Shih, D. M. (2011) Paraoxonase-2 modulates stress response of endothelial cells to oxidized phospholipids and a bacterial quorum-sensing molecule. *Arterioscler.Thromb.Vasc.Biol.* **31**, 2624-2633
27. Devarajan, A., Bourquard, N., Grijalva, V. R., Gao, F., Ganapathy, E., Verma, J., and Reddy, S. T. (2013) Role of PON2 in innate immune response in an acute infection model. *Mol.Genet.Metab*
28. Marsillach, J., Mackness, B., Mackness, M., Riu, F., Beltran, R., Joven, J., and Camps, J. (2008) Immunohistochemical analysis of paraoxonases-1, 2, and 3 expression in normal mouse tissues. *Free Radic.Biol.Med.* **45**, 146-157
29. Altenhofer, S., Witte, I., Teiber, J. F., Wilgenbus, P., Pautz, A., Li, H., Daiber, A., Witan, H., Clement, A. M., Forstermann, U., and Horke, S. (2010) One enzyme, two functions: PON2 prevents mitochondrial superoxide formation and apoptosis independent from its lactonase activity. *J.Biol.Chem.* **285**, 24398-24403
30. Schweikert, E. M., Devarajan, A., Witte, I., Wilgenbus, P., Amort, J., Forstermann, U., Shabazian, A., Grijalva, V., Shih, D. M., Farias-Eisner, R., Teiber, J. F., Reddy, S. T., and Horke, S. (2012) PON3 is upregulated in cancer tissues and protects against mitochondrial superoxide-mediated cell death. *Cell Death Differ.* **19**, 1549-1560
31. Draganov, D. I., Teiber, J. F., Speelman, A., Osawa, Y., Sunahara, R., and La Du, B. N. (2005) Human paraoxonases (PON1, PON2, and PON3) are lactonases with overlapping and distinct substrate specificities. *J.Lipid Res.* **46**, 1239-1247
32. Abas, L., and Luschnig, C. (2010) Maximum yields of microsomal-type membranes from small amounts of plant material without requiring ultracentrifugation. *Analytical biochemistry* **401**, 217-227
33. Grant, R. L., and Acosta, D. (1997) Ratiometric measurement of intracellular pH of cultured cells with BCECF in a fluorescence multi-well plate reader. *In Vitro Cell Dev.Biol.Anim* **33**, 256-260
34. Witte, I., Altenhoefer, S., Wilgenbus, P., Amorat, J., Clement, A. M., Pautz, A., Li, H., Foerstermann, U., and Horke, S. (2011) Beyond reduction of atherosclerosis: PON2 provides apoptosis resistance and stabilizes tumor cells. *Cell Death and Disease* **2**, doi:10.1038/cddis.2010.1091
35. Teiber, J. F., Draganov, D. I., and La Du, B. N. (2003) Lactonase and lactonizing activities of human serum paraoxonase (PON1) and rabbit serum PON3. *Biochem.Pharmacol.* **66**, 887-896
36. Speake, T., Yodozawa, S., and Elliott, A. C. (1998) Modulation of calcium signalling by intracellular pH in exocrine acinar cells. *Eur.J.Morphol.* **36 Suppl**, 165-169

37. Riemann, A., Schneider, B., Ihling, A., Nowak, M., Sauvant, C., Thews, O., and Gekle, M. (2011) Acidic environment leads to ROS-induced MAPK signaling in cancer cells. *PLoS.One.* **6**, e22445
38. Hagmann, H., Kuczkowski, A., Ruehl, M., Lamkemeyer, T., Brodesser, S., Horke, S., Dryer, S., Schermer, B., Benzing, T., and Brinkkoetter, P. T. (2014) Breaking the chain at the membrane: paraoxonase 2 counteracts lipid peroxidation at the plasma membrane. *FASEB journal : official publication of the Federation of American Societies for Experimental Biology* **28**, 1769-1779
39. Devarajan, A., Bourquard, N., Hama, S., Navab, M., Grijalva, V. R., Morvardi, S., Clarke, C. F., Vergnes, L., Reue, K., Teiber, J. F., and Reddy, S. T. (2011) Paraoxonase 2 deficiency alters mitochondrial function and exacerbates the development of atherosclerosis. *Antioxid.Redox.Signal.* **14**, 341-351
40. Santo-Domingo, J., and Demaurex, N. (2012) Perspectives on: SGP symposium on mitochondrial physiology and medicine: the renaissance of mitochondrial pH. *The Journal of general physiology* **139**, 415-423
41. Wahjudi, M., Papaioannou, E., Hendrawati, O., van Assen, A. H., van Merkerk, R., Cool, R. H., Poelarends, G. J., and Quax, W. J. (2011) PA0305 of Pseudomonas aeruginosa is a quorum quenching acylhomoserine lactone acylase belonging to the Ntn hydrolase superfamily. *Microbiology* **157**, 2042-2055

FIGURE LEGENDS

Figure 1

Intracellular 3OC12-acid accumulation is PON2-dependent.

(A, B) HEK and EA.hy cells were treated for shown times with 25 µM 3OC12, rinsed, extracted with acetonitrile and extracts analysed for 3OC12-acid by HPLC. (**C**) HBEC which were transfected with scrambled or PON2 siRNA for 3 days and then treated for 5 min with 25 µM 3OC12. Cells were then rinsed, extracted and analysed for 3OC12-acid. PON2 activity in scrambled and PON2 siRNA cell lysates was 16.8 ± 2.9 U/mg and 5.2 ± 0.9 U/mg, respectively (C). All data points shown represent the mean ± S.D. of 3 separate treatments.

Figure 2

3OC12-mediates intracellular acidification and Ca^{2+} rise.
(A, B) Naive EA.hy cells were loaded with Fluo-4AM and SNARF-4F and fluorescence intensities recorded in confocal time-lapse images to monitor intracellular calcium and pH fluxes, respectively, in response to 50 µM 3OC12. Green channel (A; top; Fluo-4AM) reports cytosolic Ca^{2+} rise; intensity of blue channel (A; middle; ratio of acidic / basic SNARF-4F signals) is a measure of cytosolic acidification. Scale bar, 50µm (A). Fluorescence intensities for all cells were individually measured, allowing simultaneous determination of changes in pH and Ca^{2+} within the same cell. In B, SNARF-4F ratio before 3OC12 stimulation was set as zero. Graph shows mean / S.E.M. from four representative experiments. **(C-D)** HBEC loaded with BCECF-AM to detect cytosolic pH values (C) or Fluo-4AM to detect cytosolic Ca^{2+} rise (D) were treated with increasing concentrations of 3OC12 and fluorescence measured on the microplate reader. A representative trace from four independent experiments is shown for each 3OC12 dose (C-D). The background (DMSO treated) values were subtracted from the 3OC12 treated values (C-D).

Figure 3

3OC12-mediated intracellular acidification and Ca^{2+} rise are PON2-dependent.
(A-C) Cells were loaded with BCECF-AM to detect cytosolic pH values or **(D-F)** Fluo-4AM to detect cytosolic Ca^{2+} rise and then treated with test compounds and fluorescence measured on the microplate reader. (A and D) HEK and (B and E) EA.hy 926 cells were treated with 25 µM 3OC12. (C and F) HBEC were transfected with scrambled or PON2 siRNA and three days later treated with 50 µM 3OC12 and in F, 25 µM of the phospholipase C activator m3M3FBS. PON2 activity in scrambled and PON2 siRNA cell lysates was 15.0 ± 2.9 U/mg and 1.6 ± 0.7 U/mg, respectively (C and F). All traces shown are a representative trace from at least

four independent experiments in which the background (DMSO treated) values were subtracted from the treated values.

Figure 4

3OC12-induced activation of p38 and eIF2a signalling is PON2-dependent.
(A) Primary HUVECs were treated with indicated concentrations of 3OC12 for 10 min. Subsequently, levels of total and phosphorylated p38 and eIF2a were assessed by Western blotting. Tubulin served as loading control. **(B, C)** EA.hy cells were treated with 3OC12 (or LPS) as indicated, followed by immunoblotting against phosphorylated p38 and eIF2a. **(D)** Quantitative evaluation ± SEM of p38 and eIF2a phosphorylation from four individual experiments as in B+C. **(E)** Similar experiment as in B+C, but using HUVECs that were untreated (naïve) or treated with PON2 specific or control siRNAs. **(F)** Quantitative evaluation ± SEM of four individual experiments as in (E). Values for naïve and control siRNA treated cells were the same (not shown). **(G)** HBECs treated with control or PON2 specific siRNA were incubated with 3OC12 as indicated, followed by immunoblotting for total / phosphorylated p38 and eIF2a, PON2 and α-tubulin as before. **(H)** quantification of the average ± the range of blots from two individual experiments as in (G).

Figure 5

3OC12 induces PON2-mediated mitochondrial acidification.
(A) EA.hy 926 cells were loaded with mitochondrial ratiometric pH indicator SNARF-1 (upper row; orange/red) and mitochondrial dye DiOC6 (green) as indicated in the method section. Cells were treated with 3OC12 (50 µM). $[pH]_m$ changes were observed in time-lapse 3D confocal imaging for the indicated duration. A change of SNARF1 ratiometric fluorescence from orange/red to yellow/green indicates acidification. **(B)** Quantification of $[pH]_m$ changes during 3OC12 treatment. **(C)** EA.hy 926 cells with PON2 overexpression (red curve) show an increased rate of 3OC12-induced $[pH]_m$ drop than controls (black). Each trace shows the average SNARF1 ratiometric $[pH]_m$ from 8-15 individual experiments.

Figure 6

TQ416 inhibits PON2 and prevents intracellular acidification by 3OC12.
(A) HEK PON2 cell lysates, or purified recombinant PON2 (inset), were analysed for PON2 activity in the presence of increasing concentrations of TQ416. All data points shown represent the mean ± S.D. of three separate treatments. **(B)** EA.hy PON2 cells were loaded with BCECF-AM and decreases in intracellular acidification was determined after treatment with 50 µM 3OC12 in the presence of increasing concentrations of TQ416 as described in Experimental Procedures. All traces shown are a representative trace from at least four independent experiments in which the background (DMSO treated) values were subtracted from the treated values.

Figure 1

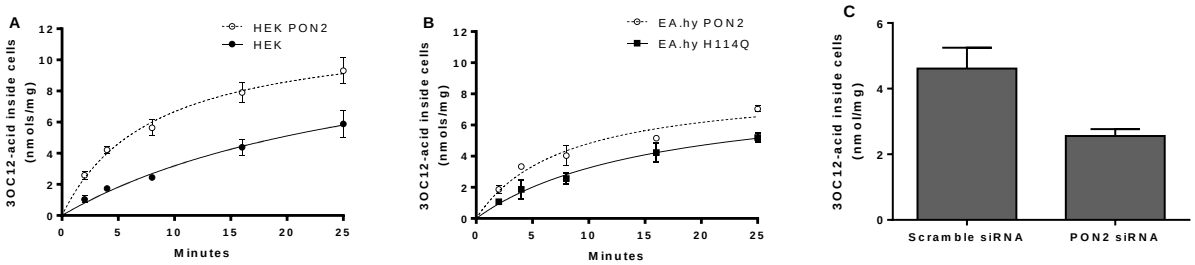

Figure 2

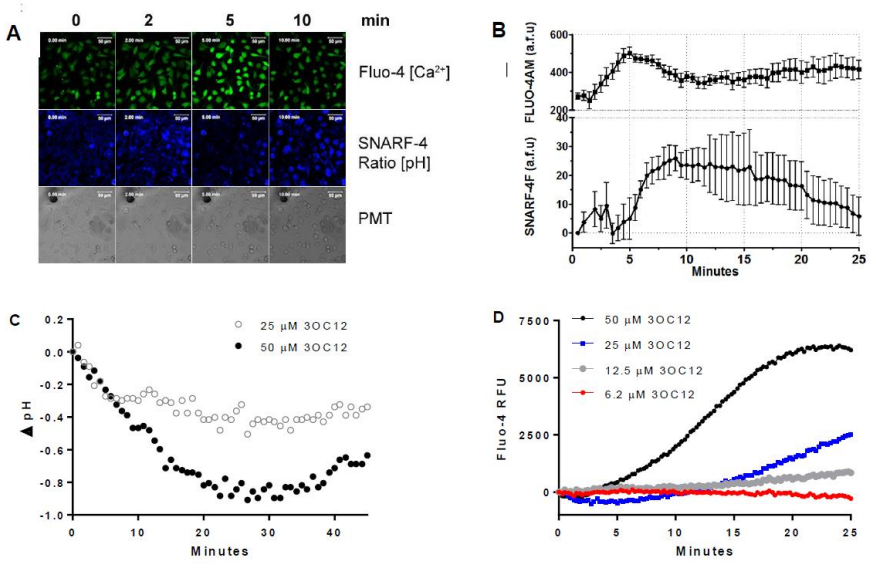

Figure 3

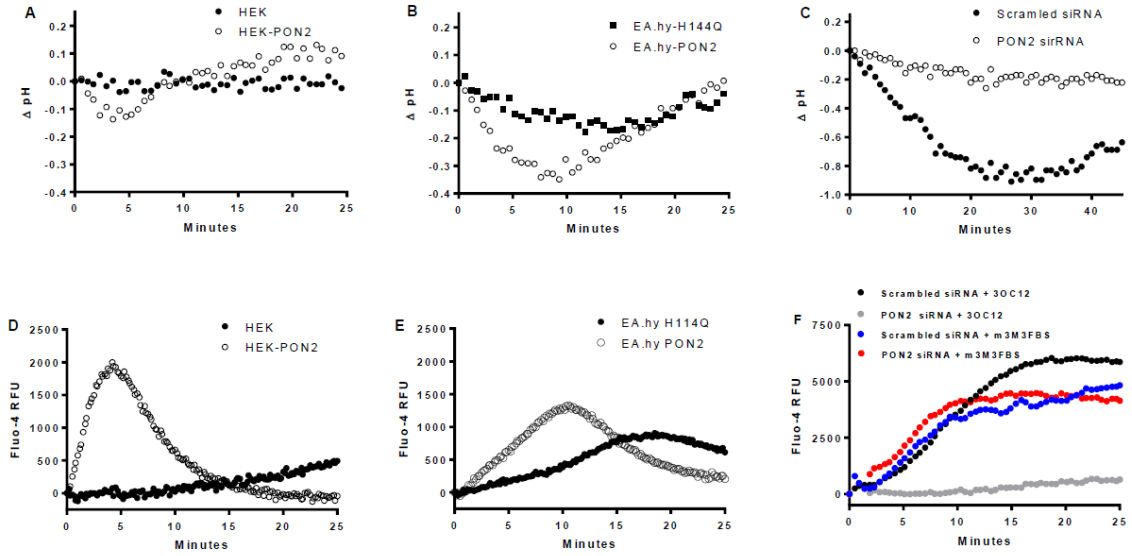

Figure 4

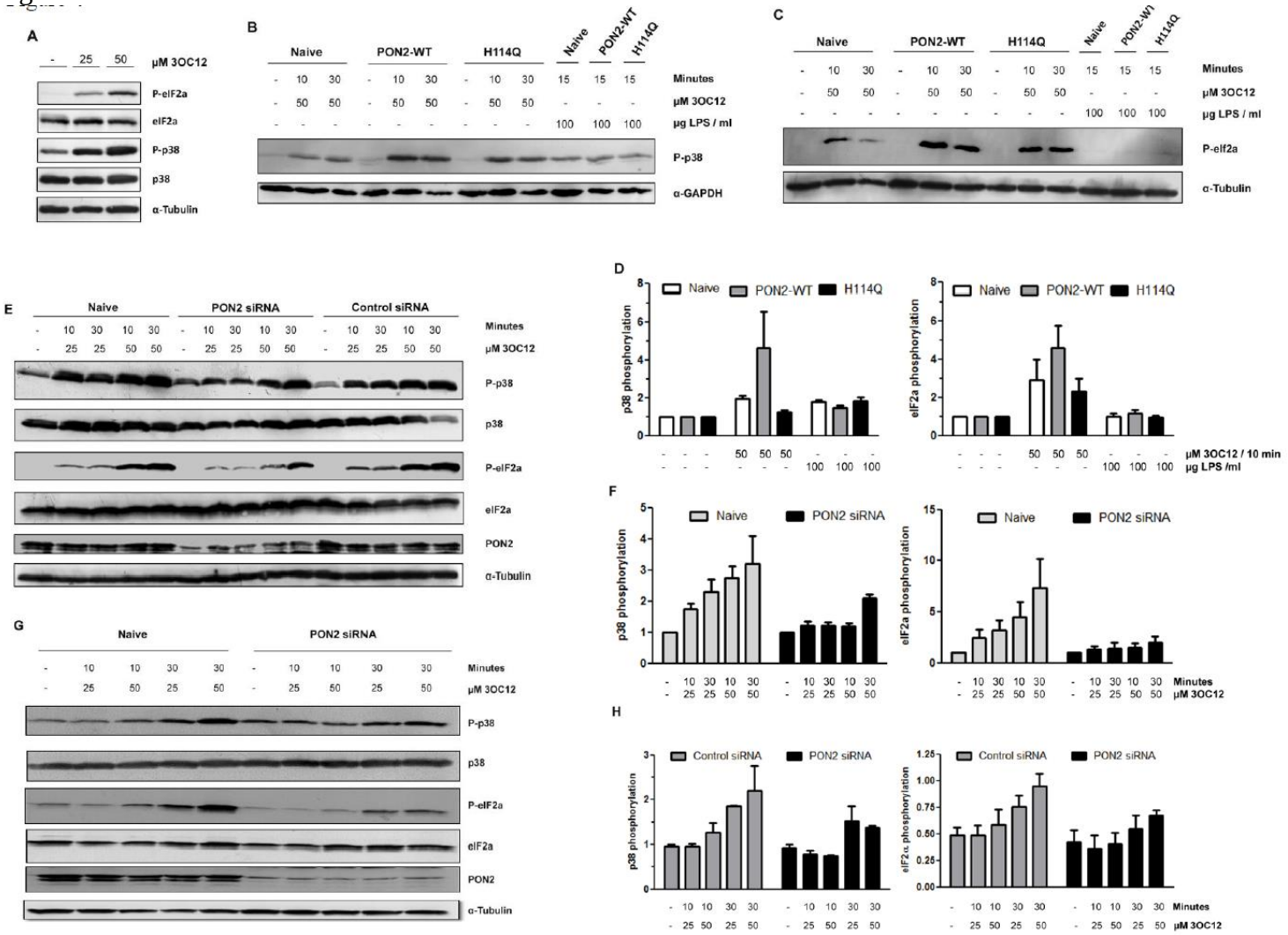
A
μM 3OC12
P-eIF2a
eIF2a
P-p38
p38
α-Tubulin
B
Naive
PON2-WT
H114Q
Minutes
μM 3OC12
μg LPS / ml
P-p38
α-GAPDH
C
Minutes
μM 3OC12
μg LPS / ml
P-eIf2a
α-Tubulin
D
Naive
PON2-WT
H114Q
p38 phosphorylation
eIF2a phosphorylation
μM 3OC12 / 10 min
μg LPS /ml
E
Naive
PON2 siRNA
Control siRNA
Minutes
μM 3OC12
P-p38
p38
P-eIF2a
eIF2a
PON2
α-Tubulin
F
Naive
PON2 siRNA
p38 phosphorylation
eIF2a phosphorylation
Minutes
μM 3OC12
G
Naive
PON2 siRNA
Minutes
μM 3OC12
P-p38
p38
P-eIF2a
eIF2a
PON2
α-Tubulin
H
Control siRNA
PON2 siRNA
p38 phosphorylation
eIF2α phosphorylation
Minutes
μM 3OC12

Figure 5

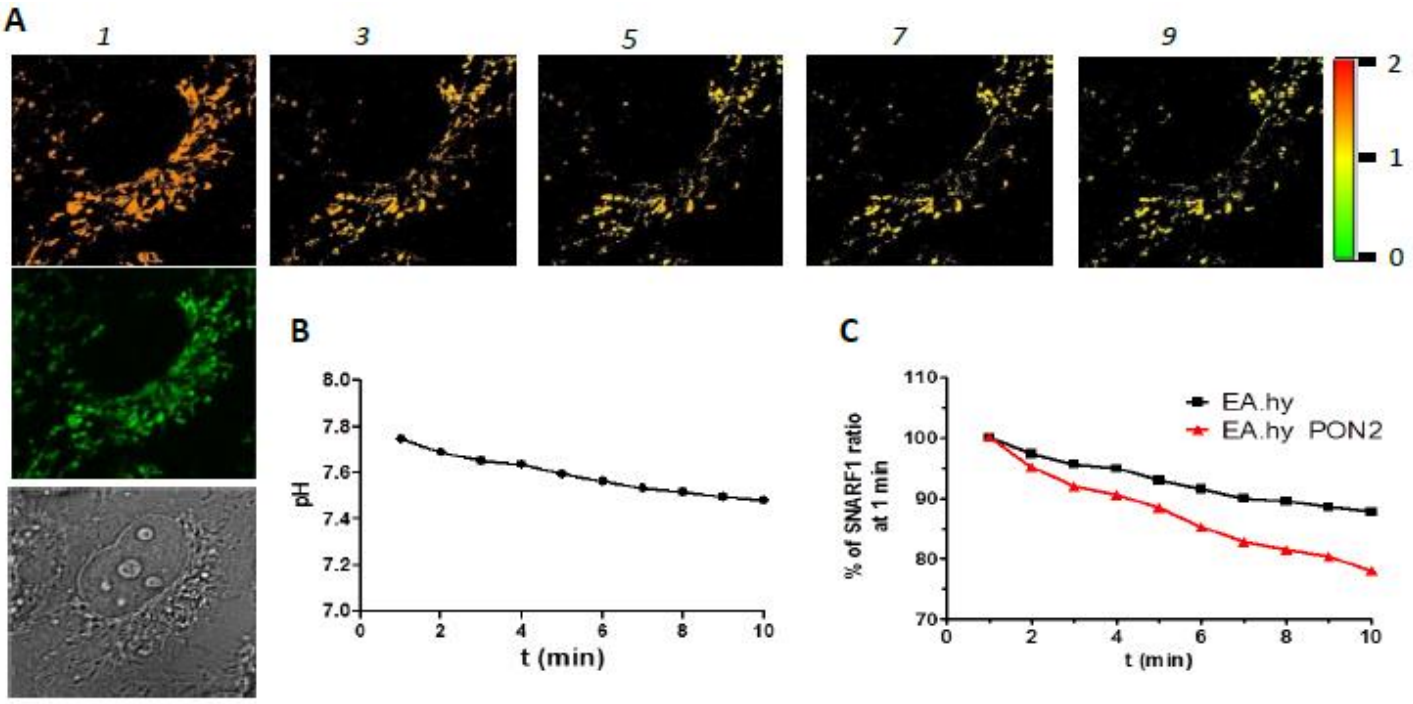

Figure 6

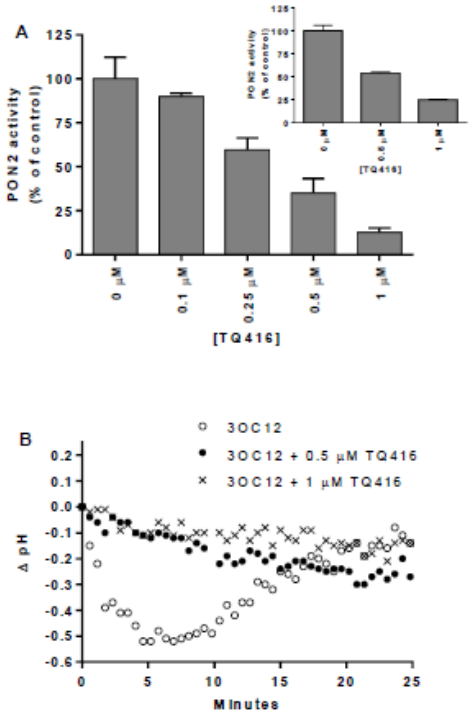

IX. Appendix II

Mass Spectrometry Analysis of the PON2 crosslinked protein complex

Submission: SUB2777 - SVJ735 Tieber 3-17
Search: MSS3225 - SVJ735 Tieber 3-17 (Meta)

Protein	Description	Length (AA)	mw (Da)	PSMs	Peptide Seqs	% Coverage
P11021	GRP78_HUMAN 78 kDa glucose-regulated protein OS=Homo sapiens GN=HSPA5 PE=1 SV=2	654	72469	181	65	64
CONT_GFP_AEQVI	Possible Contaminant GFP_AEQVI	238	26923	97	19	61
CONT_ALBU_BOVIN	Possible Contaminant ALBU_BOVIN	607	69429	91	46	64
P04264	K2C1_HUMAN Keratin, type II cytoskeletal 1 OS=Homo sapiens GN=KRT1 PE=1 SV=6	644	66179	53	39	57
P35527	K1C9_HUMAN Keratin, type I cytoskeletal 9 OS=Homo sapiens GN=KRT9 PE=1 SV=3	623	62207	48	21	54
G3V1K3	G3V1K3_HUMAN Paraoxonase 2, isoform CRA_a OS=Homo sapiens GN=PON2 PE=2 SV=1	375	38063	44	6	18
P13645	K1C10_HUMAN Keratin, type I cytoskeletal 10 OS=Homo sapiens GN=KRT10 PE=1 SV=6	584	58954	39	26	47
P11142	HSP7C_HUMAN Heat shock cognate 71 kDa protein OS=Homo sapiens GN=HSPA8 PE=1 SV=1	646	71034	36	22	33
P08107	HSP71_HUMAN Heat shock 70 kDa protein 1A/1B OS=Homo sapiens GN=HSPA1A PE=1 SV=5	641	70189	25	17	26
P39023	RL3_HUMAN 60S ribosomal protein L3 OS=Homo sapiens GN=RPL3 PE=1 SV=2	403	46188	21	14	32
P35908	K22E_HUMAN Keratin, type II cytoskeletal 2 epidermal OS=Homo sapiens GN=KRT2 PE=1 SV=2	639	65573	19	22	39
P62280	RS11_HUMAN 40S ribosomal protein S11 OS=Homo sapiens GN=RPS11 PE=1 SV=3	158	18455	16	10	53
F8W7G7	F8W7G7_HUMAN Ugl-Y3 OS=Homo sapiens GN=FN1 PE=2 SV=1	2211	247200	15	10	6
P23396	RS3_HUMAN 40S ribosomal protein S3 OS=Homo sapiens GN=RPS3 PE=1 SV=2	243	26744	15	10	44
P62829	RL23_HUMAN 60S ribosomal protein L23 OS=Homo sapiens GN=RPL23 PE=1 SV=1	140	14892	15	7	51
E9PKZ0	E9PKZ0_HUMAN 60S ribosomal protein L8 (Fragment) OS=Homo sapiens GN=RPL8 PE=2 SV=1	205	28079	14	9	35
CONT_RS27A_HUMAN	Possible Contaminant RS27A_HUMAN	156	17990	13	5	40
P49327	FAS_HUMAN Fatty acid synthase OS=Homo sapiens GN=FASN PE=1 SV=3	2511	273993	12	12	6
B4DGP8	B4DGP8_HUMAN Calnexin OS=Homo sapiens GN=CANX PE=2 SV=1	627	67688	11	7	14
CONT_ALBU_HUMAN	Possible Contaminant ALBU_HUMAN	609	69502	11	14	24
H0YEN5	H0YEN5_HUMAN 40S ribosomal protein S2 (Fragment) OS=Homo sapiens GN=RPS2 PE=2 SV=1	195	31377	11	8	37
P04843	RPN1_HUMAN Dolichyl-diphosphooligosaccharide--protein glycosyltransferase subunit 1 OS=H	607	68707	11	8	16
P36578	RL4_HUMAN 60S ribosomal protein L4 OS=Homo sapiens GN=RPL4 PE=1 SV=5	427	47794	11	7	21
P62701	RS4X_HUMAN 40S ribosomal protein S4, X isoform OS=Homo sapiens GN=RPS4X PE=1 SV=2	263	29651	11	8	26
CONT_TRYP_PIG	Possible Contaminant TRYP_PIG	231	24448	10	2	8
B4DVY7	B4DVY7_HUMAN Flotillin-1 OS=Homo sapiens GN=FLOT1 PE=2 SV=1	379	47452	10	10	23
Q86YZ3	HORN_HUMAN Hornerin OS=Homo sapiens GN=HRNR PE=1 SV=2	2850	283074	9	6	10
F8VWC5	F8VWC5_HUMAN 60S ribosomal protein L18 OS=Homo sapiens GN=RPL18 PE=2 SV=1	159	21675	9	7	42
P35232	PHB_HUMAN Prohibitin OS=Homo sapiens GN=PHB PE=1 SV=1	272	29858	9	9	43
P07437	TBB5_HUMAN Tubulin beta chain OS=Homo sapiens GN=TUBB PE=1 SV=2	444	47862	8	4	12
B5MCT8	B5MCT8_HUMAN 40S ribosomal protein S9 OS=Homo sapiens GN=RPS9 PE=2 SV=1	139	22632	7	6	26
P46779	RL28_HUMAN 60S ribosomal protein L28 OS=Homo sapiens GN=RPL28 PE=1 SV=3	137	15774	7	7	39
Q00839	HNRPU_HUMAN Heterogeneous nuclear ribonucleoprotein U OS=Homo sapiens GN=HNRNPU P	825	89158	7	7	10
Q02878	RL6_HUMAN 60S ribosomal protein L6 OS=Homo sapiens GN=RPL6 PE=1 SV=3	288	32780	7	5	19
P62241	RS8_HUMAN 40S ribosomal protein S8 OS=Homo sapiens GN=RPS8 PE=1 SV=2	208	21920	6	4	30
P10412	H14_HUMAN Histone H1.4 OS=Homo sapiens GN=HIST1H1E PE=1 SV=2	219	21406	6	3	18
P14625	ENPL_HUMAN Endoplasmin OS=Homo sapiens GN=HSP90B1 PE=1 SV=1	803	92646	6	6	10
P62277	RS13_HUMAN 40S ribosomal protein S13 OS=Homo sapiens GN=RPS13 PE=1 SV=2	151	17248	6	5	34
Q00610	CLH1_HUMAN Clathrin heavy chain 1 OS=Homo sapiens GN=CLTC PE=1 SV=5	1675	188257	6	5	4
C9JNW5	C9JNW5_HUMAN 60S ribosomal protein L24 OS=Homo sapiens GN=RPL24 PE=2 SV=1	150	17804	5	4	35
H0YMV8	H0YMV8_HUMAN 40S ribosomal protein S27 OS=Homo sapiens GN=RPS27L PE=2 SV=1	100	9489	5	2	25
P13647	K2C5_HUMAN Keratin, type II cytoskeletal 5 OS=Homo sapiens GN=KRT5 PE=1 SV=3	590	62502	5	12	19
P08238	HS90B_HUMAN Heat shock protein HSP 90-beta OS=Homo sapiens GN=HSP90AB1 PE=1 SV=4	724	83428	5	4	9
P19338	NUCL_HUMAN Nucleolin OS=Homo sapiens GN=NCL PE=1 SV=3	710	76767	5	4	8
P25705	ATPA_HUMAN ATP synthase subunit alpha, mitochondrial OS=Homo sapiens GN=ATP5A1 PE=1 S	553	54604	5	5	13
P26373	RL13_HUMAN 60S ribosomal protein L13 OS=Homo sapiens GN=RPL13 PE=1 SV=4	211	24301	5	4	15
P02533	K1C14_HUMAN Keratin, type I cytoskeletal 14 OS=Homo sapiens GN=KRT14 PE=1 SV=4	472	51656	5	12	26
P62269	RS18_HUMAN 40S ribosomal protein S18 OS=Homo sapiens GN=RPS18 PE=1 SV=3	152	17744	5	3	18
P62753	RS6_HUMAN 40S ribosomal protein S6 OS=Homo sapiens GN=RPS6 PE=1 SV=1	249	28735	5	3	15
P68104	EF1A1_HUMAN Elongation factor 1-alpha 1 OS=Homo sapiens GN=EEF1A1 PE=1 SV=1	462	50279	5	4	11
P07996	TSP1_HUMAN Thrombospondin-1 OS=Homo sapiens GN=THBS1 PE=1 SV=2	1170	129642	4	3	3
P22626	ROA2_HUMAN Heterogeneous nuclear ribonucleoproteins A2/B1 OS=Homo sapiens GN=HNRNP	353	36074	4	4	13
A5A3E0	POTEF_HUMAN POTE ankyrin domain family member F OS=Homo sapiens GN=POTEF PE=1 SV=2	1075	121592	4	2	9
A8MUD9	A8MUD9_HUMAN 60S ribosomal protein L7 OS=Homo sapiens GN=RPL7 PE=2 SV=1	208	29279	4	4	25
B4DY08	B4DY08_HUMAN Heterogeneous nuclear ribonucleoproteins C1/C2 OS=Homo sapiens GN=HNRN	288	27877	4	3	19
E7EMK3	E7EMK3_HUMAN Flotillin-2 OS=Homo sapiens GN=FLOT2 PE=2 SV=1	483	47161	4	3	10

Appendix II Continued

E7EWT1	E7EWT1_HUMAN Dolichyl-diphosphooligosaccharide--protein glycosyltransferase 48 kDa subun	419	50895	4	3	8
F5GY37	F5GY37_HUMAN Prohibitin-2 OS=Homo sapiens GN=PHB2 PE=2 SV=1	267	33348	4	4	18
J3KTE4	J3KTE4_HUMAN Ribosomal protein L19 OS=Homo sapiens GN=RPL19 PE=2 SV=1	194	23505	4	3	14
M0QYS1	M0QYS1_HUMAN 60S ribosomal protein L13a (Fragment) OS=Homo sapiens GN=RPL13A PE=2 SV	210	23616	4	4	20
M0R117	M0R117_HUMAN 60S ribosomal protein L18a OS=Homo sapiens GN=RPL18A PE=2 SV=1	154	20785	4	4	21
O15118	NPC1_HUMAN Niemann-Pick C1 protein OS=Homo sapiens GN=NPC1 PE=1 SV=2	1278	142452	4	2	2
P01857	IGHG1_HUMAN Ig gamma-1 chain C region OS=Homo sapiens GN=IGHG1 PE=1 SV=1	330	41368	4	2	5
P04259	K2C6B_HUMAN Keratin, type II cytoskeletal 6B OS=Homo sapiens GN=KRT6B PE=1 SV=5	564	60192	4	13	23
D6R9I7	D6R9I7_HUMAN 40S ribosomal protein S23 OS=Homo sapiens GN=RPS23 PE=2 SV=1	123	15834	3	2	35
P62854	RS26_HUMAN 40S ribosomal protein S26 OS=Homo sapiens GN=RPS26 PE=1 SV=3	115	13012	3	2	14
A2AEA2	A2AEA2_HUMAN HLA class I histocompatibility antigen, Cw-14 alpha chain OS=Homo sapiens GN	372	40518	3	2	7
P01892	1A02_HUMAN HLA class I histocompatibility antigen, A-2 alpha chain OS=Homo sapiens GN=HLA	365	41321	3	2	7
B4DEM7	B4DEM7_HUMAN T-complex protein 1 subunit theta OS=Homo sapiens GN=CCT8 PE=2 SV=1	529	59745	3	3	8
B4E2W0	B4E2W0_HUMAN 3-ketoacyl-CoA thiolase OS=Homo sapiens GN=HADHB PE=2 SV=1	452	51388	3	3	6
Q92945	FUBP2_HUMAN Far upstream element-binding protein 2 OS=Homo sapiens GN=KHSRP PE=1 SV=	711	73268	3	2	3
E7EQV9	E7EQV9_HUMAN Ribosomal protein L15 (Fragment) OS=Homo sapiens GN=RPL15 PE=2 SV=1	174	24185	3	2	10
Q9H0U3	MAGT1_HUMAN Magnesium transporter protein 1 OS=Homo sapiens GN=MAGT1 PE=1 SV=1	335	38102	2	2	6
CONT_PRDX1_HUMAN	Possible Contaminant PRDX1_HUMAN	199	22150	2	2	12
F8VPV9	F8VPV9_HUMAN ATP synthase subunit beta OS=Homo sapiens GN=ATP5B PE=2 SV=1	518	56669	2	3	9
G3V0E5	G3V0E5_HUMAN Transferrin receptor (P90, CD71), isoform CRA_c OS=Homo sapiens GN=TFRC PE	679	85034	2	2	4
P62424	RL7A_HUMAN 60S ribosomal protein L7a OS=Homo sapiens GN=RPL7A PE=1 SV=2	266	30049	2	5	20
P62913	RL11_HUMAN 60S ribosomal protein L11 OS=Homo sapiens GN=RPL11 PE=1 SV=2	178	14950	2	2	18
H0Y2W2	H0Y2W2_HUMAN ATPase family AAA domain-containing protein 3A (Fragment) OS=Homo sapie	572	58056	2	2	6
P04350	TBB4A_HUMAN Tubulin beta-4A chain OS=Homo sapiens GN=TUBB4A PE=1 SV=2	444	49870	1	3	9
P08779	K1C16_HUMAN Keratin, type I cytoskeletal 16 OS=Homo sapiens GN=KRT16 PE=1 SV=4	473	51362	1	10	18
E7EPB3	E7EPB3_HUMAN 60S ribosomal protein L14 OS=Homo sapiens GN=RPL14 PE=2 SV=1	124	23471	1	2	16

X. Supporting Data

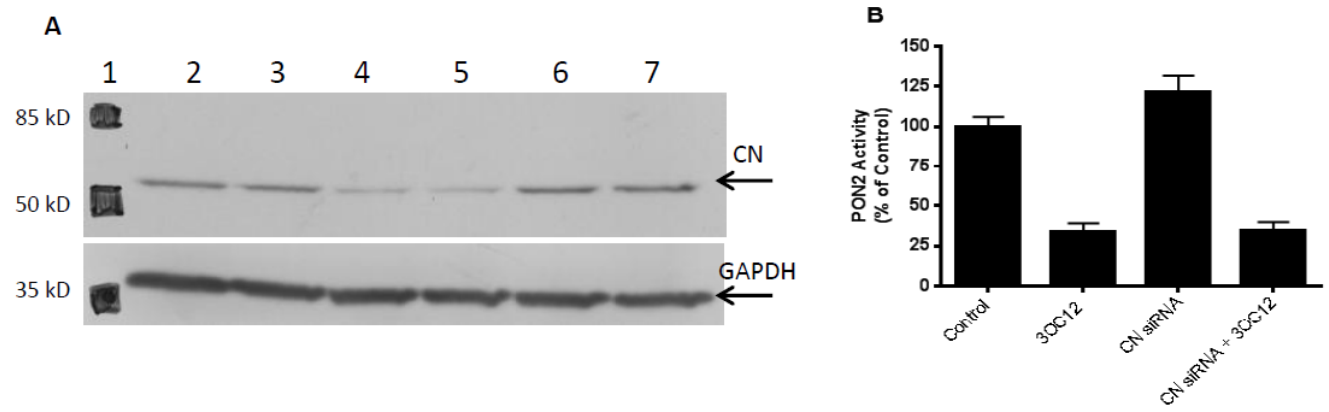

Figure 1 **Effect of blocking calcineurin on cellular PON2 activity.** EA.hy 926 cells were transfected with 10 nM CN siRNA or a control siRNA (using Synvolux, NL transfection reagent). Two days later, cells were either left untreated or treated with 75 μM 3OC12 for 10 min. (A) CN and GAPDH expression in lysed cells was determined by immunobloting with a anti-human CN and GAPDH antibody, respectively. Lane 1- protein standards, lane 2- non-transfected; lane 3- 3OC12 only; lane 4- CN siRNA; lane 5- CN siRNA+ 3OC12; lane 6- control siRNA; lane 7- control siRNA + 3OC12. (B) PON2 activity in cell lysates transfected with siRNAs and treated with or without 3OC12. The experiments were done in duplicate and error bars represent the range.

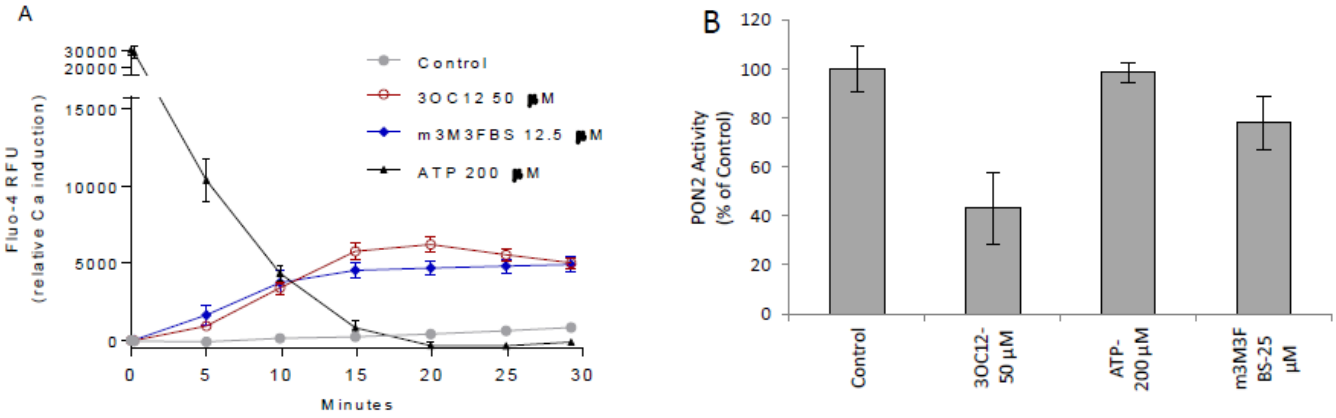

Figure 2 **Inactivation of PON2 in HBEC treated with calcium inducers.** (A) HBEC cells plated at 25,000 per well in 96 well plates were loaded the next day with the calcium indicator fluo-4 AM, treated with the calcium inducers and fluorescence monitored on a fluorescence plate reader. (B) HBEC cells plated at 75,000 per well on 24 well plates were treated the next day with the calcium inducers for 20 min. Cells were then collected, rinsed and lysed and lysates analyzed for PON2 activity. Each point or bar represents the average of triplicate experiments and the error bars represent the SDs.

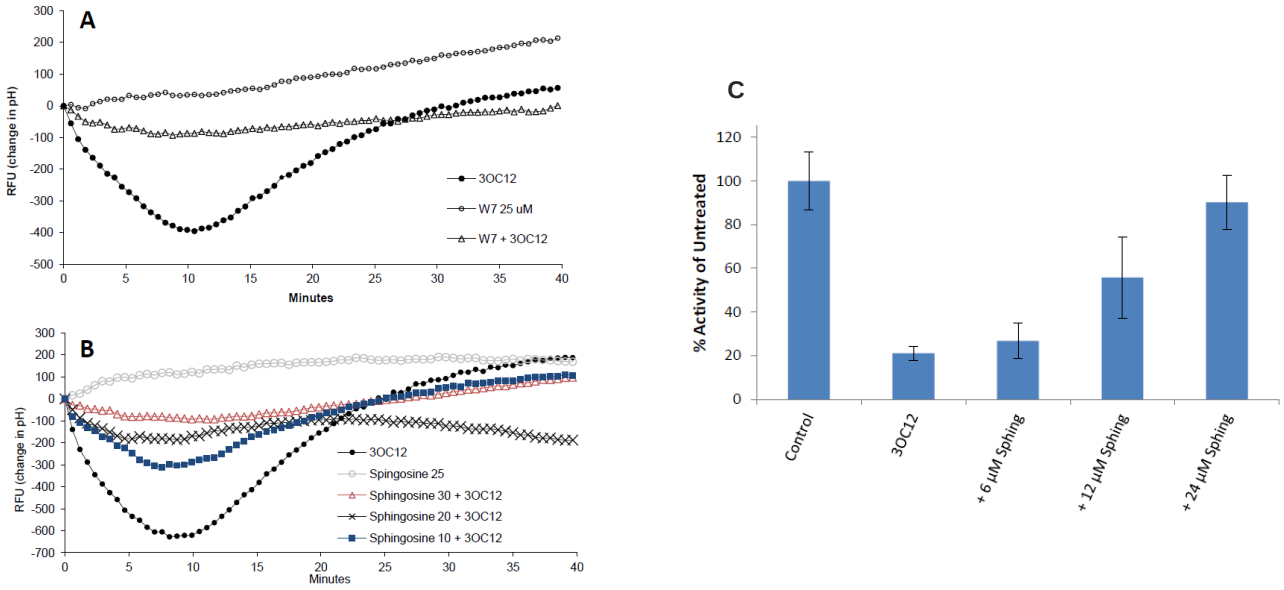

Figure 3. Amphipathic weak bases prevent 3OC12-mediated intracellular acidification and PON2 inactivation. EA.hy 926 PON2-GFP were plated at 25,000 per well on 96 well plates. The following day, the cells were loaded with 2.5 µM BCECF, rinsed and treated with DMSO (solvent for W7 and sphingosine stocks) or W7 (A) or sphingosine (B) at shown concetrations for 20 minutes. The cells were then treated without or with 50 µM 3OC12 in the presence of the inhibitors and fluorescence recorded for 40 min. (C) A549 cells plated at 75,000 per well on 24 well plates were pre-treated for 20 min with sphingosine followed by at 10 min treatment with 50 µM 3OC12, in the presence of sphingosine. Cells were collected, rinsed and lysed and lysates analyzed for PON2 activity. Experiments were performed in triplicate and error bars represent the coefficients of variation.

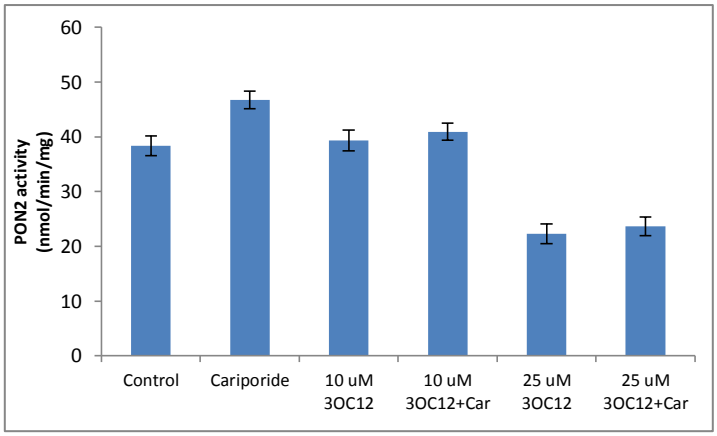

Figure 4. The Na+/H+ exchange inhibitor cariporide does not potentiate PON2 inactivation. A549 cells were plated at 75,000 per well on 24 well plates and the next day treated with cariporide. One hour later that cells were treated with cariporide + 3OC12 for 10 minutes and then cells were washed, lysed and analyzed for PON2 activity. Experiments were performed in triplicate and error bars represent the SDs.

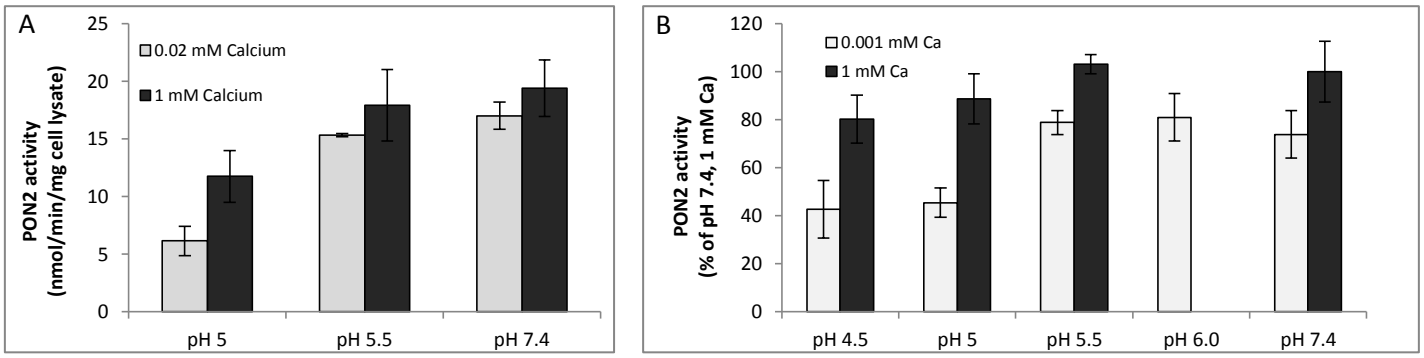

Figure 5. pH and Calcium-dependent inactivation of PON2. A549 cell lysates were pre-incubated with 0.02 mM (A) and 0.001 mM (B) calcium at the shown pH values for 10 minutes. Lysates were then analyzed for PON2 activity, with 3OC12 as the substrate, in standard pH 7.4 reaction buffer containing 1 mM $CaCl_2$ to determine the extent of irreversible inactivation or "denaturing" of PON2. Each bar represents the average of duplicate or triplicate experiments and the error bars represent the SDs (in A) and CVs (in B).

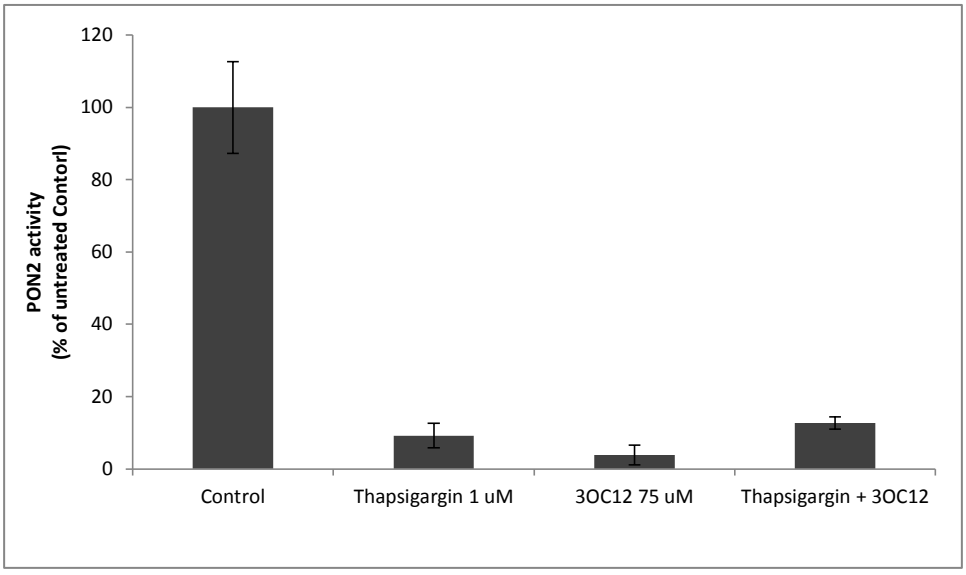

Figure 6. Thapsigargin inactivates PON2. A549 cells were plated at 50,000 per well on 24 well plates and the next day treated with thapsigargin or 3OC12 for 15 minutes or preteated with thapsigargin for 15 minutes followed by treatment with 3OC12 for 10 minutes. Cells were then washed, lysed and analyzed for PON2 activity. Experiments were performed in triplicate and error bars represent the CVs.

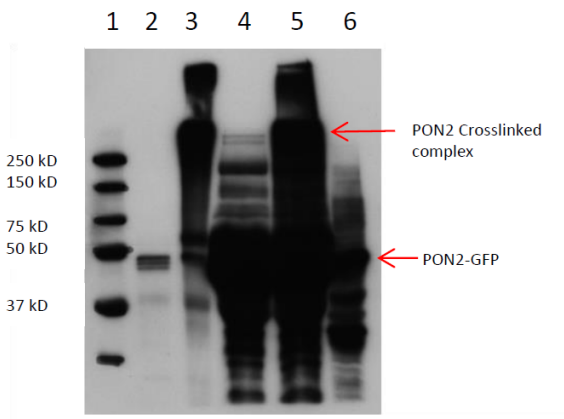

Figure 7 (left). PON2 immunoblot of the IP of the crosslinked PON2-GFP protein complex. HEK-PON2-GFP cells were left untreated or treated with 100 μM 3OC12 for 15 min and then lysed and treated with or without BS^3 crosslinker. The lysates were then IPed with an anti-rabbit human PON2 antibody using Dynabeads, washed, separated by SDS-PAGE, transferred to a membrane and immunoblotted with a mouse anti-human PON2 antibody. Lane 1-standards, lane 2-IP PON2 from crosslinked untreated cells, lane 3- IP PON2 from crosslinked 3OC12 treated cells, lane 4- IP supernatant from crosslinked untreated cells, lane 5- IP supernatant from crosslinked 3OC12 treated cells, lane 6- non-crosslinked cell lysate.

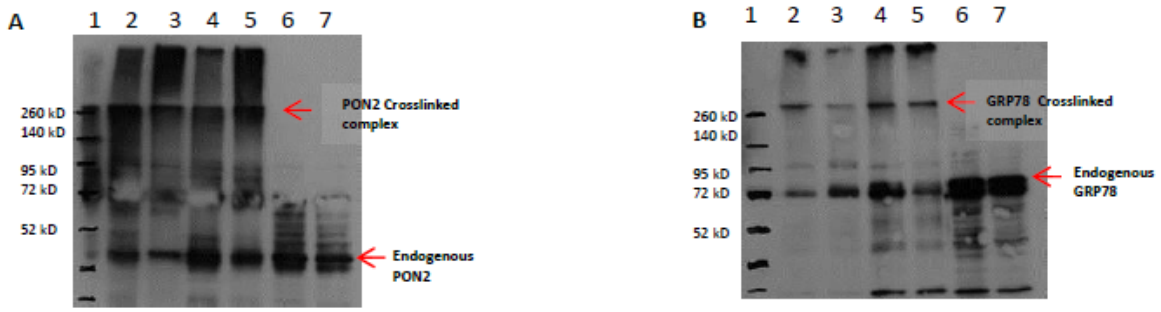

Figure 8. Western Analysis of Crosslinking of GRP78 and PON2. (A) PON2 and (B) GRP78 immunoblots of HEK-PON2 cell lysates from cells left untreated or treated with 3OC12 to inactivate PON2, crosslinked with BS^3 and then analyzed by SDS-PAGE. Lane 1, standards; lanes 2 and 4, untreated cells; lanes 3 and 5, 3OC12 treated cells; lane 6, untreated cells not crosslikned; lane 7, 3OC12 treated cells not crosslinked.

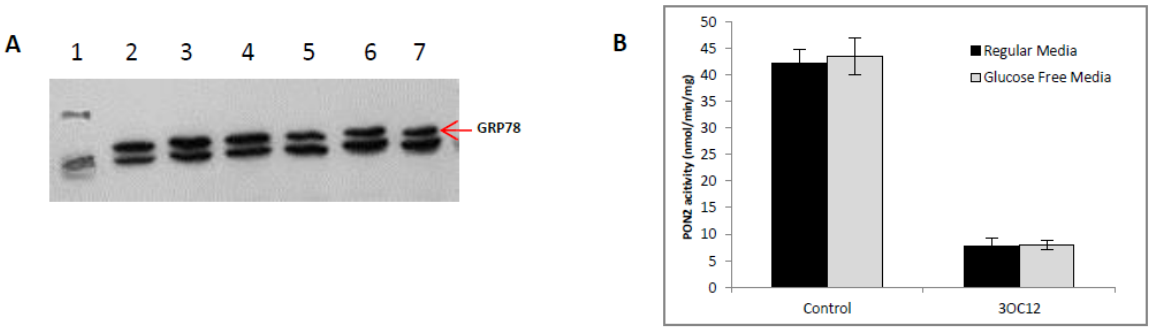

Figure 9. Increased GRP78 expression does not protect PON2 from inactivation. (A) GRP78 Western blot lysates from A549 cells. Lane 1, standards; Lanes 2-4, glucose free media; lanes 5-7, regular media. The upper band is GRP78, denoted by the arrow. (B) PON2 activity was determined in A549 cell lysates from cells grown for 24 hrs in regular or glucose free media and then treated with or without (control) 100 μM 3OC12 for 10 minutes.

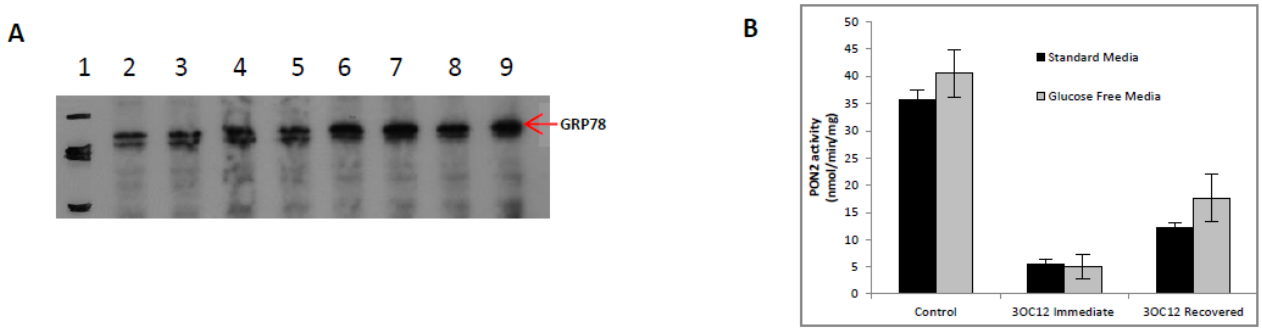

Figure 10. Increased GRP78 expression does promote PON2 recovery. (A) GRP78 Western blot lysates from A549 cells. Lane 1, standards; Lanes 2-5, regular media; lanes 6-9, glucose free media. (B) PON2 activity was determined in A549 cell lysates from cells grown for 24 hrs in standard or glucose free media and then treated without (control) or with 100 μM 3OC12 for 10 minutes and then analyzed immediately or analyzed after 3 hrs.

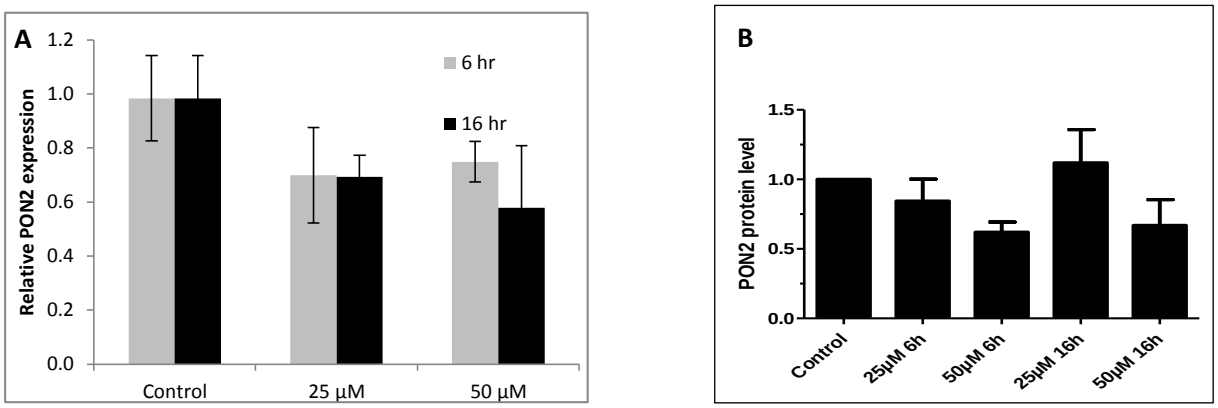

Figure 11. 3OC12 down-regulates PON2 mRNA and protein in HBEC. HBEC cell were plated at 75,000 cell per well in 24 well plates. The next day fresh media was added without (control) or with 3OC12. mRNA levels were determine by real time RT-PCR of cell lysates (A). PON2 mRNA levels were normalized to the housekeeping gene beta-actin. PON2 protein levels were determined by Western analysis (B). Experiments were performed in triplication and error bars represent the SDs.

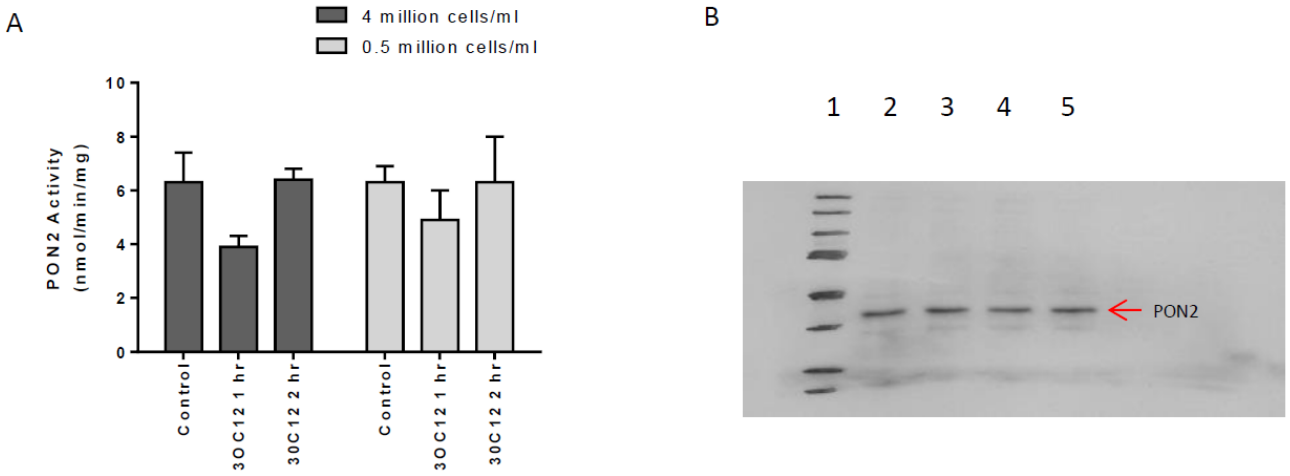

Figure 12. 3OC12 mediate PON2 inactivation in mouse spleen cells. (A) Cells were isolated from mouse spleen and incubated in DMEM containing 10 % FBS with or without 100 µM 3OC12. After the given times, cells were washed, lysed and analyzed for PON2 activity. All assays were performed in triplicate and the error bars represent the SD. (B) Western analysis of PON2 in mouse spleen cell lysates, immunoblotted with a mouse PON2 specific antibody (GenTex). Lane 1, ladder; lane 2-5, lysates from 4 different spleen cell pellets.

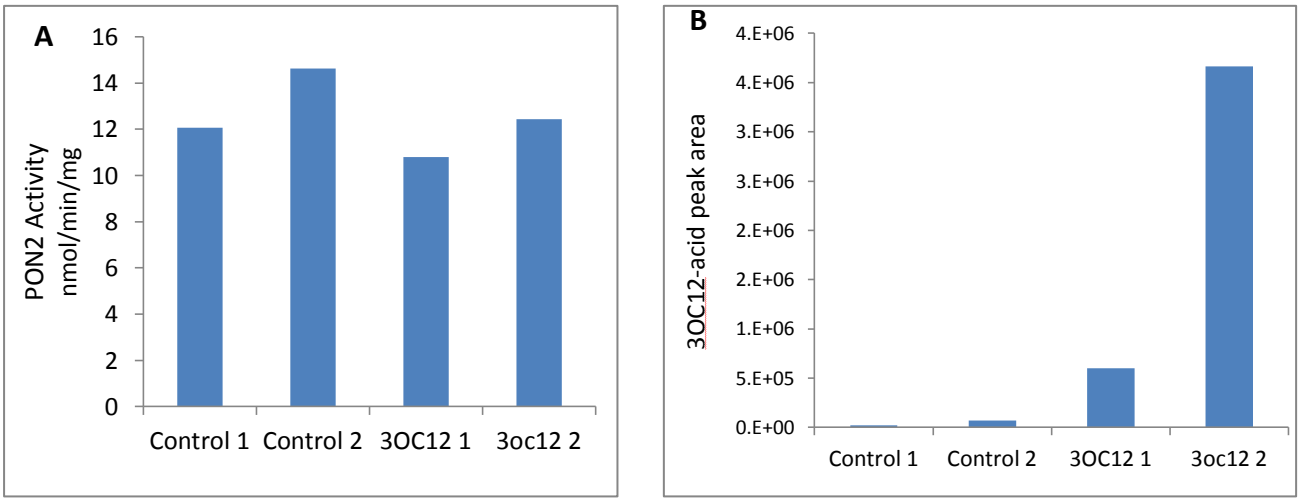

Figure 13. Ex vivo perfusion of mouse lung with 3OC12. Mouse lungs were perfused through the left ventricle and also filled with media without (control) or with 200 µM of 3OC12 for 1 hour. (A) Sections of the treated lungs were analyzed for PON2 hydrolytic activity. (B) Sections of the treated lungs were extracted with acetonitrile and ethyl acetate. After drying the solvent the samples were treated with the carboxylic acid conjugating agent PDAM in ethyl acetate and 3OC12-acid analyzed by HPLC.

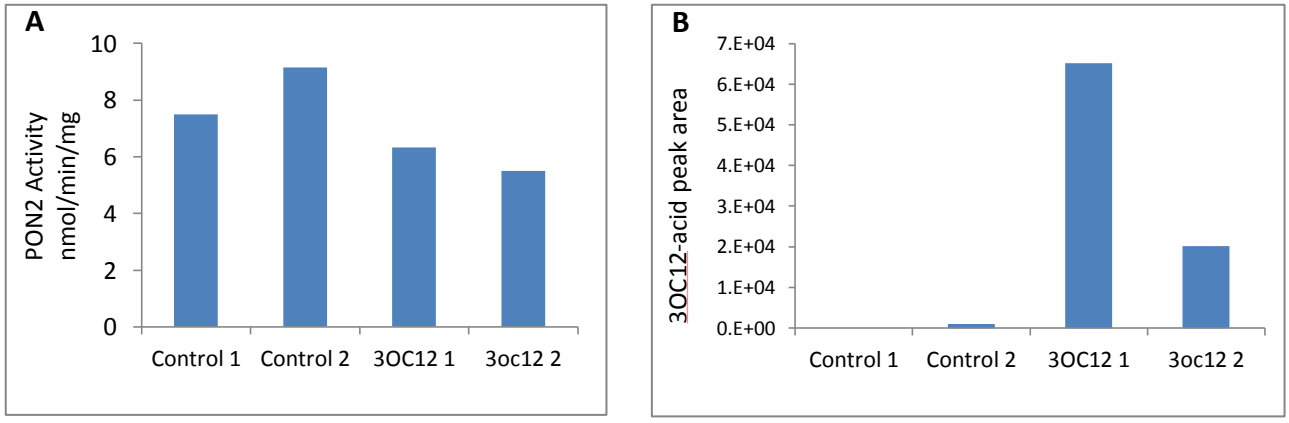

Figure 14. Ex vivo perfusion of mouse liver with 3OC12. Mouse livers were perfused through inferior vena cava with 20 ml of media without (control) or with 200 µM of 3OC12. (A) Sections of the treated livers were analyzed for PON2 hydrolytic activity. (B) Sections of the treated livers were extracted with acetonitrile and ethyl acetate. After drying the solvent the samples were treated with the carboxylic acid conjugating agent PDAM in ethyl acetate and 3OC12-acid analyzed by HPLC.

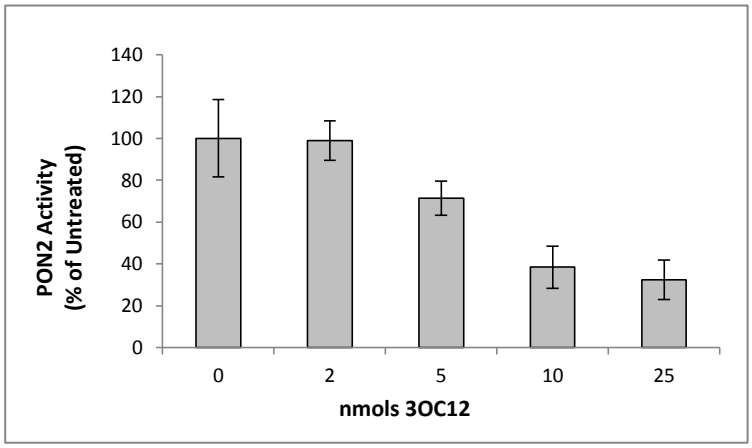

Figure 15. Dependence of PON2 inactivation on the amount of 3OC12. HEK-PON2-GFP cells were suspended in media containing 100 µM 3OC12 at increasing volumes of media, resulting in increasing total nmols of 3OC12, for 10 minutes. Cells were then pelleted, washed and lysed and lysates analyzed for PON2 activity. Assays were performed in triplicated and error bars represent the CVs.

Maintenance of Paraoxonase 2 Activity as a Strategy to Attenuate P. Aeruginosa Virulence.

Award Number: DM110018 W81XWH-12-2-0091

PI: John Teiber **Org:** The University of Texas Southwestern Medical Center **Award Amount:** $643,615.00

Study Aims

- Identify the mechanism(s) and signaling pathways that mediate inactivation of PON2 by the bacterial virulence molecule 3OC12.
- Characterize the ability of 3OC12 to down-regulate PON2 in primary cell types relevant to *P. aeruginosa* infections.
- Demonstrate the feasibility of blocking the 3OC12-mediated inactivation/down-regulation of PON2 in primary cells and in vivo.

Approach

To identify the mechanism(s) of PON2 inactivation we employed mass spectrometry analysis of PON2 to identify protein modification(s), PON2 site-directed mutagenesis studies and inhibitors and inhibitory RNA studies targeting signaling pathways/proteins to identify PON2 inactivating signaling pathways. The sensitivity of PON2 to 3OC12-mediated inactivation is studied in primary human cell types and in mice models in vivo. Test compounds/drugs will tested in cells and in mice to determine if prevention of 3OC12-mediated PON2 inactivation could be a viable therapeutic strategy.

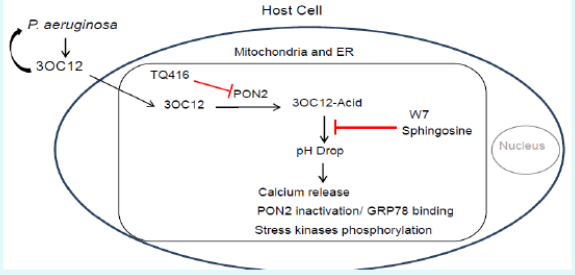

Scheme. Summary of pathways, mechanisms and inhibitors that mediate and modulate 3OC12 biological effects discovered through year 2. Preventing intracellular acidification (e.g. by W7 or sphingosine) may be a therapeutic strategy to prevent both PON2 inactivation and immunomodulatory effects of 3OC12. TQ416 may be an important inhibitor which could be used to identify the role PON2 plays in *P. aeruginosa* virulence by blocking PON2 hydrolysis of 3OC12 in mouse infection models.

Accomplishments:

- Determined that PON2 interacting proteins likely mediate 3OC12-mediated inactivation.
- Demonstrated PON2-dependent 3OC12-acid ER and mitochondrial accumulation and acidification and kinase activation in human primary bronchial epithelial cells.

Timeline and Cost

Activities FY	13	14
Mass spec and mutational analysis to identify PON2 modifications.		
Inhibition and siRNA studies to identify signaling pathways that mediate PON2 inactivation.		
PON2 inactivation/downregulation in primary cells and in mice.		
Blocking PON2 inactivation primary cells and in mice.		
Estimated Budget ($K)	**$321**	**$321**

Updated: (October 1, 2014)

Milestones

FY14 Goals – Identify signaling pathways/mechanisms that inactivate PON2

☑ Identified inhibitors that prevent PON2 inactivation and 3OC12 bio-effects.

☑ Identified binding of interacting proteins to PON2 as likely inactivation mechanism.

FY14 Goals – Characterize 3OC12-mediated PON2 inactivation/down-regulation in primary cells.

☑ Characterized pathways and sensitivity in HBECs.

☑ Mouse spleen cells insensitive to 3OC12-mediated inactivation

FY14 Goals – Characterize PON2 inactivation and 3OC12-acid accumulation in mice.

☑ Currently no in vivo inactivation detected.

☑ In vivo intracellular accumulation of 3OC12-acid in lung tissues occurres.

Comments/Challenges

- Inactivation of PON2 in vivo (mice) is not effective due to non-receptor mechanism of 3OC12. New approaches to evaluate 3OC12 and *P. aeruginosa*-mediated PON2 inactivation are being developed.
- Under budget primarily because divisional funds from other sources were available that needed to be spent in FY13.

Budget Expenditure to Date

Projected Expenditure: $ 643,615.00

Actual Expenditure: $ 492,920.00